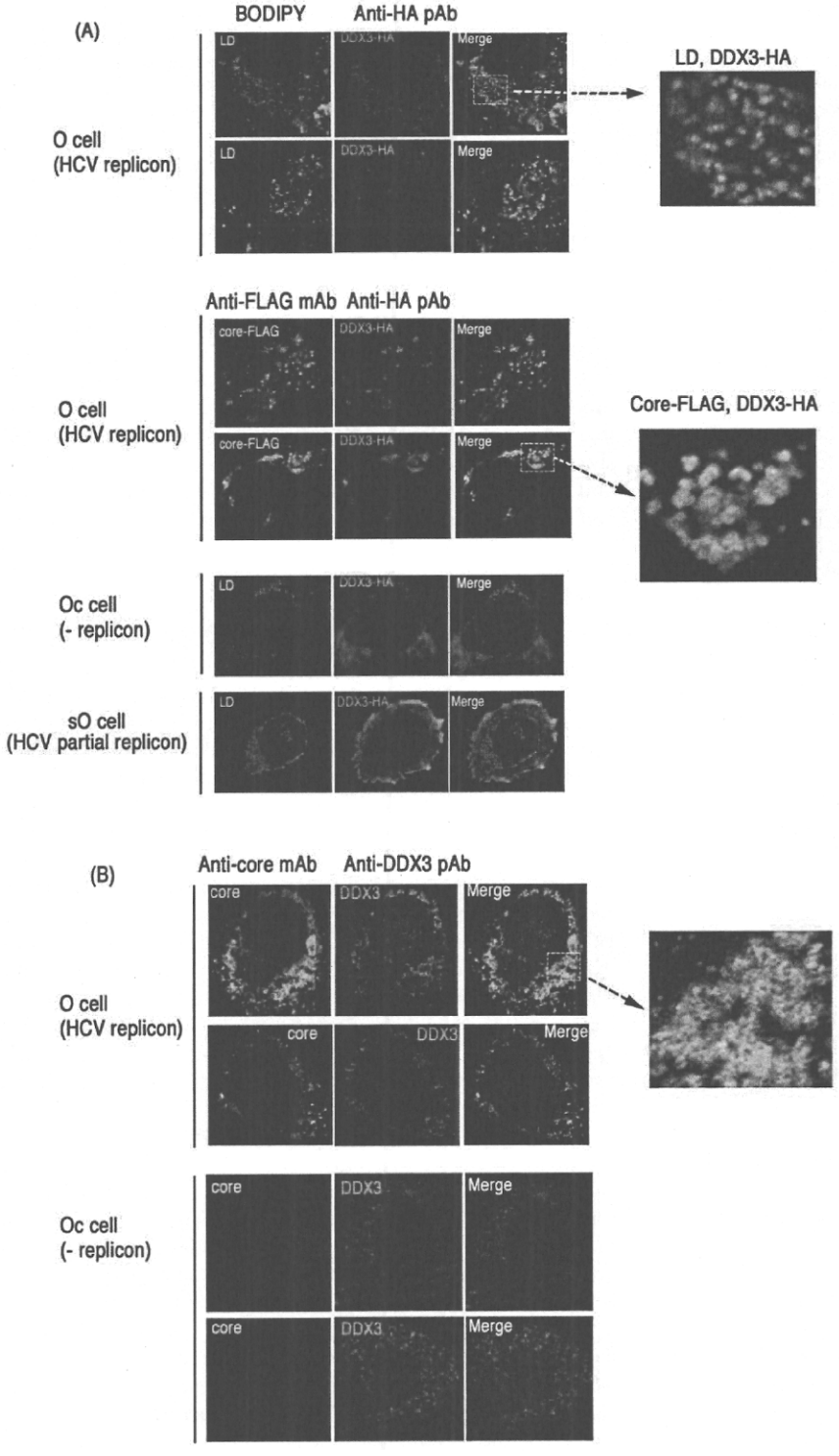

Figure 7. Partial association of endogenous and overexpressed DDX3 with HCV core protein in hepatocyte lines. (A) O cells with the HCV replicon form DDX3-containing speckles in the cytoplasm. O cells contain full-length HCV replicon, and Oc cells do not [16]. O cells were transfected with a plasmid expressing HA-tagged DDX3 (top panel). In other experiments, O cells were transfected with plasmids expressing HA-tagged DDX3 and FLAG-tagged HCV core protein (center panel). After 24 hrs, cells were stained with anti-HA or FLAG antibodies. Proteins were visualized with Alexa488 or 564 second antibodies and the LD was stained with BODIPY493/503. In the bottom panel, Oc cells (no replicon) and sO cells with the core-less subgenomic replicon [16] were transfected with a plasmid expressing HA-tagged DDX3. After 24 hrs, cells were stained with anti-HA antibodies. LD was stained with BODIPY493/503. (B) Endogenous DDX3-HCV core association in O cells. O or Oc cells were cultured to amplify the HCV replicon. Cells were stained with anti-core mAb and anti-DDX3pAb and secondary antibodies. Similar sets of experiments were performed three times to confirm the results.
doi:10.1371/journal.pone.0014258.g007

GDF3 promotes turmorigenesis. The secondary effect of GDF3 expression on other genes should not be ruled out. One possible hypothesis is that GDF3 expression leads to an increase of some genes in CSC-like cells and these cells have a strong tumorigenic activity thus contributing to high GDF3 tumortigenicity.

Yamanaka and his colleagues firstly showed that the expression of four ES-specific genes, Klf4, Oct3/4, Sox2, and c-Myc, induces pluripotent stem cell proliferation from mouse embryonic and adult fibroblast cultures [10]. Another report also showed that another ES-specific gene Sall4 plays a positive role in the generation of pluripotent stem cells from blastocysts and fibroblasts [33]. In the current CSC theory, CSCs are derived from normal stem cells. Although several papers support this model, it is still unknown whether all CSCs are derived from normal stem cells [13]. In general, cancer cell genome becomes unstable because caretaker tumor suppressor genes are mutated during carcinogenesis [34]. Genome instability causes the expression of genes that are suppressed in normal tissues. In human ES cells, GDF3 supports the maintenance of the stem cell markers, Oct4, Nanog, and Sox2 [8,9]. Therefore, it is possible that some fraction of cancer cells may come to express these four genes *in vivo* leading to CSC formation from differentiated cancer cells, and GDF3 may promote this process. Another possibility of GDF3 role in tumorigensis is that GDF3 modulates TGF-mediated signaling, since it belongs to the TGF-β superfamily [8]. However, this model cannot explain why GDF3 expression increased only CD24 expression and not Id1 expression.

CD24 is a GPI-anchored sialoglycoprotein and is expressed in a variety of malignant cells [35]. CD24 participates in cell-cell contact and cell-matrix interaction and plays a role in cell proliferation. It is currently accepted that absence of CD24 on the tumor cell surface inhibits proliferative response and induces apoptosis in tumor cells, while up-regulation of CD24 promotes cell proliferation to increase tumor growth and metastasis [35,36]. Thus, the high CD24 level on tumor cells may predict poor prognosis in patients with cancer. In hepatocellular carcinoma CD24 level is actually correlated with patients' prognosis [36]. Our present finding furthers this notion and suggests that constitutive or forced expression of GDF3 in melanoma cells links the high CD24 expression accelerating tumor growth. By what mechanism TGF-β-like GDF3 induces up-regulation of CD24 on tumor cells, however, remains unknown.

In this regard, ectopic expression of GDF3 did not promote tumorigenesis of mouse hepatoma G1 and G5 cells. The expression profiles of CD24 in B16 melanoma sublines were parallel to those of GDF3, but hepatoma lines G1 and G5 had impaired the ability to induce GDF3-mediated CD24 expression. CD24 is rarely expressed on normal cells. Only limited subsets of myeloid cells are CD24-positive [36]. As the signal axis of this GDF3-derived CD24-inducing pathway is undetermined, it remains unsettled as to what is the molecular discrepancy between B16 F1/F10 melanoma cells and G-1/G5 hepatoma cells. Furthermore, the physiological role of the GDF3 signal and its downstream targets has not been elucidated. Yet the GDF3-CD24 pathway frequently turns positive when the cells are malignantly transformed [37] which may support the notion that CD24, when complexed with other molecules, alters its function for discrimination of danger signals [37].

Although possible experiments are in progress, another report suggests that CD24 is associated with Siglec-10 in humans or Siglec-G in mice serve as an innate immune receptor for endogenous self ligands named damage associated molecular pattern (DAMP) [38]. Accumulating evidence indicates that in tumor progression DAMP is released from damaged tissue or tumor cells and modulates both tumor and immune cells. Recent report suggested that the host inflammatory response to DAMP is partly controlled by a DAMP-CD24-Siglec axis [38]. We favor the speculation that the CD24 signals the presence of DAMP in a tumor micro environment, thereby augmenting inflammatory response to facilitate pathological tumor progression in GDF3-CD24 pathway-positive B16 F1/F10 but not -negative G-1/G-5 cells. Either way, this is the first report on the embryonic antigen GDF3 which is an inducer of CD24 and joins tumor cell proliferation. Further study may clarify the link between the CD24-Siglec G pathway and innate inflammatory response which occurs in invading tumor and facilitates to establish tumorigenesis.

Materials and methods

Cell lines and mice

B16-F1 and B16-F10 melanoma cells, G1 and G5 hepatoma cells were grown in RPMI1640 with 10% fetal bovine serum. These cell lines were transfectable, and transfection efficiencies were checked using the pEFBOS vector for expression of GFP. The transfection efficiencies were ~25% in F1 and F10 cells and ~20% in G-1 and G-5 cells (data not shown). We tried to establish stable clones constitutively expressing GDF3 in F1 and F10 cells, but failed to establish them. C57BL/6 and BALB/c mice (10-20 weeks of age) were purchased from Hokudo Co. (Sapporo, Japan). All mice were maintained under specific pathogen-free conditions in the animal facility of the Hokkaido University Graduate School of Medicine. Animal experiments were performed according to the guidelines set by the animal safety center, Japan.

RT-PCR

Total RNA from cells, tumors and normal tissues was isolated using the TRIZOL reagent (Invitrogen) according to the manufacturer's standard instructions. Reverse transcription was performed with random primers using the High Capacity cDNA reverse transcription kit (ABI). PCR was performed using primers listed in Table 1. These primer sets are applicable to the detection of the messages in mouse ES cells [10]. PCR cycles were usually 35 rounds, and otherwise described. We avoided quantitative interpretation of the results of RT-PCR analysis. The amplified DNA fragments were analyzed with 1% agarose gel and stained with etidium bromide.

Quantitative PCR

We used the following PCR primers: GDF3-F1, GDF3-R1, β-actin-F1, and β-actin R1 for quantitative PCR. Their sequences for GDF3 gene are listed in Table 1, and those of β-actin are a follows: β-actin-F1: TTT GCA GCT CCT TCG TTG C, and β-actin-R1: TCG TCA TCC ATG GCG AAC T. Quantitative PCR was performed by Step One real-time PCR system (ABI). The statistical comparisons were performed using the Student's *t* test between two groups.

Table 1 Primer sequences

Primer name	Primer sequence (F: forward)	Primer sequence (R: reverse)
Dppa2	agaagccgtgcaaagaaaaa	gttaaaatgcaacgggctgt
Fthl17	actttgggactgtgggactg	ttgatagcatcctcgcactg
Sall4	gcccctcaactgtctctctg	gggagctgtttttctccactg
Rex1	caggttctggaagcgagttc	gacaagcatgtgcttcctca
Utf1	ttacgagcaccgacactctg	cgaaggaacctcgtagatgc
Tcl1	caccatgagggacaagacct	cttacaccgctctgcaatca
Sox2	atgggctctgtggtcaagtc	ccctcccaattcccttgtat
Dppa3	ctttgttgtcggtgctgaaa	tcccgttcaaactcatttcc
Gdf3	acctttccaagatggctcct	cctgaaccacagacagagca
Ecat8	tgtgtactggcaaccaaaa	ctgaggtcccatcagctctc
Dnmt3l	caagcctcgtgactttcctc	ccatggcattgatcctctct
Eras	atcctaacccccaactgtcc	caagcctcgtgactttcctc
Fbxol5	ctatgattggctgcgacaga	gtagtgtcgggaggcaatgt
Dppa5	cagtcgctggtgctgaaata	tccatttagcccgaatcttg
Ecatl	gaatgcctggaagatccaaa	aaatctcagctcgcctttca
Dppa4	agggctttcccagaacaaat	gcaggtatctgctcctctgg
Soxl5	cggcgtaagagcaaaaactc	tgggatcactctgagggaag
Oct3/4	ccaatcagcttgggctagag	ctgggaaaggtgtccctgta
Nanog	cacccacccatgctagtctt	accctcaaactcctggtcct
c-Myc	gcccagtgaggatatcttgga	atcgcagatgaagctctggt
Grb2	tcaatgggaaagatggcttc	gagcatttcttctgccttgg
β-catenin	gtgcaattcctgagctgaca	cttaaagatggccagcaagc
Stat3	agactacaggccctcagcaa	cctctgtcaggaaaggcttg
CD133	ctcatgcttgagagatcaggc	cgttgaggaagatgtgcacc
CD24	actctcacttgaaattgggc	gcacatgttaattactagtaaagg
CD44	gaaaggcatcttatggatgtgc	ctgtagtgaaacacaacacc
ABCB5	gtggctgaagaagccttgtc	tgaagccgtagccctcttta
GDF3	aaatgtttgtgttgcggtca	tctggcacaggtgtcttcag

Tumor transplantation

B16 melanoma cells or G1, G5 hepatoma cells were cultured in 10-cm dishes and harvested with 0.02% EDTA solution. Cells were washed two times with D-PBS. Mice were anesthetized with diethyl ether and tumor cells were injected subcutaneously into C57BL/6 or BALB/c mice. Tumor volumes were measured using a caliper every 1 or 2 days. Tumor volume was calculated using the formula: Tumor volume (cm^3) = (long diameter) × (short diameter) × (short diameter) × 0.4. Plotted data represent mean ± standard deviation (SD.).

Flow cytometry

Flow cytometry (FACS) was performed using FACS caliber. Excised B16-F1 and B16-F10 tumors were treated with collagenase D for 30 minutes and then suspended in RPMI 1640 medium. Cells were washed two times with FACS buffer (1 × PBS, 1% BSA, 2 mM EDTA). 1 × 10^6 cells were suspended in 50 μl of FACS buffer. Anti mouse CD22 and CD 44 mouse antibody (eBioscience) were added into the cell suspension, and the cells were incubated at 4°C for 45 minutes. After the incubation cells were washed twice with PBS, and analyzed by FACS caliber.

Western blot analysis

Cells were lysed in lysis buffer (20 mM Tris-HCl pH7.4, 150 mM NaCl, 1% NP-40, 10 mM EDTA, 25 mM iodoacetamide, 2 mM PMSF, protease inhibitor mixture (Roche)) and subjected to SDS-PAGE (8~10% gel) under reducing conditions followed by immunoblotting with anti-mouse GDF3 mAb or anti-β actin mAb (R&D Systems, Inc., Minneapolis, MN).

Acknowledgements

We thank Drs. T. Ebihara, H. Takaki. J. Kasamatsu, A. Watanabe, and H. Shime in our laboratory for their valuable discussions. Thanks are also due to Dr. Vijaya Lakshmi for her nice discussion and English review of the manuscript. This project was supported by Grants-in-Aid from the Ministry of Education, Science and Culture and the Ministry of Health, Labor, and Welfare of Japan, Mitsubishi Foundation, Mochida Foundation, NorthTec Foundation and Yakult Foundation.

Author details

[1]Department of Microbiology and Immunology, Graduate School of Medicine, Hokkaido University, Kita-15, Nishi-7, Kita-ku Sapporo 060-8638, Japan. [2]Department of Gastroenterology, Graduate School of Medicine, Hokkaido University, Kita-15, Nishi-7, Kita-ku Sapporo 060-8638, Japan.

Authors' contributions

HO, MM and TS designed the experiments. HO and NE carried out most of the experiments. TK and MA assigned this study to our laboratory. HO and TS wrote the manuscript. All authors read and approved the final manuscript.

Competing interests
The authors declare that they have no competing interests.

Received: 28 August 2010 Accepted: 15 October 2010
Published: 15 October 2010

References

1. Jones CM, Simon-Chazottes D, Guenet JL, Hogan BL: **Isolation of Vgr-2, a novel member of the transforming growth factor-beta-related gene family.** *Mol Endocrinol* 1992, **61**:1961-1968.
2. McPherron AC, Lee SJ: **GDF-3 and GDF-9: two new members of the transforming growth factor-beta superfamily containing a novel pattern of cysteines.** *J Biol Chem* 1993, **268**:3444-3449.
3. Caricasole AA, van Schaik RH, Zeinstra LM, Wierikx CD, van Gurp RJ, van den Pol M, Looijenga LH, Oosterhuis JW, Pera MF, Ward A, de Bruijn D, Kramer P, de Jong FH, van den Eijnden-van Raaij AJ: **Human growth-differentiation factor 3 (hGDF3): developmental regulation in human teratocarcinoma cell lines and expression in primary testicular germ cell tumours.** *Oncogene* 1998, **16**:95-103.
4. Ezeh UI, Turek PJ, Reijo RA, Clark AT: **Human embryonic stem cell genes OCT4, NANOG, STELLAR, and GDF3 are expressed in both seminoma and breast carcinoma.** *Cancer* 2005, **104**:2255-2265.
5. Skotheim RI, Autio R, Lind GE, Kraggerud SM, Andrews PW, Monni O, Kallioniemi O, Lothe RA: **Novel genomic aberrations in testicular germ cell tumors by array-CGH, and associated gene expression changes.** *Cell Oncol* 2006, **28**:315-326.
6. Gopalan A, Dhall D, Olgac S, Fine SW, Korkola JE, Houldsworth J, Chaganti RS, Bosl GJ, Reuter VE, Tickoo SK: **Testicular mixed germ cell tumors: a morphological and immunohistochemical study using stem cell markers, OCT3/4, SOX2 and GDF3, with emphasis on morphologically difficult-to-classify areas.** *Mod Pathol* 2009, **22**:1066-1074.
7. Clark AT, Rodriguez RT, Bodnar MS, Abeyta MJ, Cedars MI, Turek PJ, Firpo MT, Reijo Pera RA: **Human STELLAR, NANOG, and GDF3 genes are expressed in pluripotent cells and map to chromosome 12p13, a hotspot for teratocarcinoma.** *Stem Cells* 2004, **22**:169-179.
8. Levine AJ, Brivanlou AH: **GDF3 at the crossroads of TGF-beta signaling.** *Cell Cycle* 2006, **5**:1069-1073.
9. Levine AJ, Brivanlou AH: **GDF3, a BMP inhibitor, regulates cell fate in stem cells and early embryos.** *Development* 2006, **133**:209-216.
10. Takahashi K, Yamanaka S: **Induction of pluripotent stem cells from mouse embryonic and adult fibroblast cultures by defined factors.** *Cell* 2006, **126**:663-676.
11. Chen C, Ware SM, Sato A, Houston-Hawkins DE, Habas R, Matzuk MM, Shen MM, Brown CW: **The Vg1-related protein Gdf3 acts in a Nodal signaling pathway in the pre-gastrulation mouse embryo.** *Development* 2006, **133**:319-329.
12. Lapidot T, Sirard C, Vormoor J, Murdoch B, Hoang T, Caceres-Cortes J, Minden M, Paterson B, Caligiuri MA, Dick JE: **A cell initiating human acute myeloid leukaemia after transplantation into SCID mice.** *Nature* 1994, **367**:645-648.
13. Visvader JE, Lindeman GJ: **Cancer stem cells in solid tumours: accumulating evidence and unresolved questions.** *Nat Rev Cancer* 2008, **8**:755-768.
14. Schatton T, Murphy GF, Frank NY, Yamaura K, Waaga-Gasser AM, Gasser M, Zhan Q, Jordan S, Duncan LM, Weishaupt C, Fuhlbrigge RC, Kupper TS, Sayegh MH, Frank MH: **Identification of cells initiating human melanomas.** *Nature* 2008, **451**:345-349.
15. Quintana E, Shackleton M, Sabel MS, Fullen DR, Johnson TM, Morrison SJ: **Efficient tumour formation by single human melanoma cells.** *Nature* 2008, **456**:593-598.
16. Dou J, Pan M, Wen P, Li Y, Tang Q, Chu L, Zhao F, Jiang C, Hu W, Hu K, Gu N: **Isolation and identification of cancer stem-like cells from murine melanoma cell lines.** *Cell Mol Immunol* 2007, **4**:467-472.
17. Zhong Y, Guan K, Zhou C, Ma W, Wang D, Zhang Y, Zhang S: **Cancer stem cells sustaining the growth of mouse melanoma are not rare.** *Cancer Lett* 2010, **292**:17-23.
18. Cui W, Kong NR, Ma Y, Amin HM, Lai R, Chai L: **Differential expression of the novel oncogene, SALL4, in lymphoma, plasma cell myeloma, and acute lymphoblastic leukemia.** *Mod Pathol* 2006, **19**:1585-1592.
19. Ma Y, Cui W, Yang J, Qu J, Di C, Amin HM, Lai R, Ritz J, Krause DS, Chai L: **SALL4, a novel oncogene, is constitutively expressed in human acute myeloid leukemia (AML) and induces AML in transgenic mice.** *Blood* 2006, **108**:2726-2735.
20. Zhao W, Hisamuddin IM, Nandan MO, Babbin BA, Lamb NE, Yang VW: **Identification of Kruppel-like factor 4 as a potential tumor suppressor gene in colorectal cancer.** *Oncogene* 2004, **23**:395-402.
21. Wei D, Gong W, Kanai M, Schlunk C, Wang L, Yao JC, Wu TT, Huang S, Xie K: **Drastic down-regulation of Kruppel-like factor 4 expression is critical in human gastric cancer development and progression.** *Cancer Res* 2005, **65**:2746-2754.
22. Ohnishi S, Ohnami S, Laub F, Aoki K, Suzuki K, Kanai Y, Haga K, Asaka M, Ramirez F, Yoshida T: **Downregulation and growth inhibitory effect of epithelial-type Kruppel-like transcription factor KLF4, but not KLF5, in bladder cancer.** *Biochem Biophys Res Commun* 2003, **308**:251-256.
23. Dang DT, Chen X, Feng J, Torbenson M, Dang LH, Yang VW: **Overexpression of Kruppel-like factor 4 in the human colon cancer cell line RKO leads to reduced tumorigenecity.** *Oncogene* 2003, **22**:3424-3430.
24. Pandya AY, Talley LI, Frost AR, Fitzgerald TJ, Trivedi V, Chakravarthy M, Chhieng DC, Grizzle WE, Engler JA, Krontiras H, Bland KI, LoBuglio AF, Lobo-Ruppert SM, Ruppert JM: **Nuclear localization of KLF4 is associated with an aggressive phenotype in early-stage breast cancer.** *Clin Cancer Res* 2004, **10**:2709-2719.
25. Chen YJ, Wu CY, Chang CC, Ma CJ, Li MC, Chen CM: **Nuclear Kruppel-like factor 4 expression is associated with human skin squamous cell carcinoma progression and metastasis.** *Cancer Biol Ther* 2008, **7**:777-782.
26. Foster KW, Liu Z, Nail CD, Li X, Fitzgerald TJ, Bailey SK, Frost AR, Louro ID, Townes TM, Paterson AJ, Kudlow JE, Lobo-Ruppert SM, Ruppert JM: **Induction of KLF4 in basal keratinocytes blocks the proliferation-differentiation switch and initiates squamous epithelial dysplasia.** *Oncogene* 2005, **24**:1491-1500.
27. Ying QL, Nichols J, Chambers I, Smith A: **BMP induction of Id proteins suppresses differentiation and sustains embryonic stem cell self-renewal in collaboration with STAT3.** *Cell* 2003, **115**:281-292.
28. Giubellino A, Burke TR Jr: **Bottaro DP. Grb2 signaling in cell motility and cancer.** *Expert Opin Ther Targets* 2008, **12**:1021-1033.
29. Saeki Y, Seya T, Hazeki K, Ui M, Hazeki O, Akedo H: **Involvement of phosphoinositide 3-kinase in regulation of adhesive activity of highly metastatic hepatoma cells.** *J Biochem* 1998, **124**:1020-1025.
30. Kang Y, Chen CR, Massague J: **A self-enabling TGFbeta response coupled to stress signaling: Smad engages stress response factor ATF3 for Id1 repression in epithelial cells.** *Mol Cell* 2003, **11**:915-926.
31. Schindl M, Schoppmann SF, Strobel T, Heinzl H, Leisser C, Horvat R, Birner P: **Level of Id-1 protein expression correlates with poor differentiation, enhanced malignant potential, and more aggressive clinical behavior of epithelial ovarian tumors.** *Clin Cancer Res* 2003, **9**:779-785.
32. Ito A, Watabe K, Koma Y, Kitamura Y: **An attempt to isolate genes responsible for spontaneous and experimental metastasis in the mouse model.** *Histol Histopathol* 2002, **17**:951-959.
33. Tsubooka N, Ichisaka T, Okita K, Takahashi K, Nakagawa M, Yamanaka S: **Roles of Sall4 in the generation of pluripotent stem cells from blastocysts and fibroblasts.** *Genes Cells* 2009, **14**:683-694.
34. Levitt NC, Hickson ID: **Caretaker tumour suppressor genes that defend genome integrity.** *Trends Mol Med* 2002, **8**:179-186.
35. Kristiansen G, Winzer KJ, Mayordomo E, Bellach J, Schluns K, Denkert C, Dahl E, Pilarsky C, Altevogt P, Guski H, Dietel M: **CD24 expression is a new prognostic marker in breast cancer.** *Clin Cancer Res* 2003, **9**:4906-4913.
36. Yang XR, Xu Y, Yu B, Zhou J, Li JC, Qiu SJ, Shi YH, Wang XY, Dai Z, Shi GM, Wu B, Wu LM, Yang GH, Zhang BH, Qin WX, Fan J: **CD24 is a novel predictor for poor prognosis of hepatocellular carcinoma after surgery.** *Clin Cancer Res* 2009, **15**:5518-5527.
37. Liu Y, Chen GY, Zheng P: **CD24-Siglec G/10 discriminates danger- from pathogen-associated molecular patterns.** *Trends Immunol* 2009, **30**:557-561.
38. Chen GY, Tang J, Zheng P, Liu Y: **CD24 and Siglec-10 selectively repress tissue damage-induced immune responses.** *Science* 2009, **323**:1722-1725.

doi:10.1186/1756-9966-29-135
Cite this article as: Ehira *et al.*: **An embryo-specific expressing TGF-β family protein, growth-differentiation factor 3 (GDF3), augments progression of B16 melanoma.** *Journal of Experimental & Clinical Cancer Research* 2010 **29**:135.

Published November 8, 2010

JEM

Article

Identification of a polyI:C-inducible membrane protein that participates in dendritic cell–mediated natural killer cell activation

Takashi Ebihara,[1] Masahiro Azuma,[1] Hiroyuki Oshiumi,[1] Jun Kasamatsu,[1] Kazuya Iwabuchi,[2] Kenji Matsumoto,[3] Hirohisa Saito,[3] Tadatsugu Taniguchi,[4] Misako Matsumoto,[1] and Tsukasa Seya[1]

[1]Department of Microbiology and Immunology, Hokkaido University Graduate School of Medicine, Kita-ku, Sapporo 060-8638, Japan
[2]Division of Immunobiology, Institute for Genetic Medicine, Hokkaido University, Sapporo, Japan, 060-0815, Japan
[3]Department of Allergy and Immunology, National Research Institute for Child Health and Development, Setagaya-ku, Tokyo 157-8535, Japan
[4]Department of Immunology, Graduate School of Medicine and Faculty of Medicine, University of Tokyo, Bunkyo-ku, Tokyo 113-0033, Japan

In myeloid dendritic cells (mDCs), TLR3 is expressed in the endosomal membrane and interacts with the adaptor toll/interleukin 1 receptor homology domain–containing adaptor molecule 1 (TICAM-1; TRIF). TICAM-1 signals culminate in interferon (IFN) regulatory factor (IRF) 3 activation. Co-culture of mDC pretreated with the TLR3 ligand polyI:C and natural killer (NK) cells resulted in NK cell activation. This activation was triggered by cell-to-cell contact but not cytokines. Using expression profiling and gain/loss-of-function analyses of mDC genes, we tried to identify a TICAM-1–inducing membrane protein that participates in mDC-mediated NK activation. Of the nine candidates screened, one contained a tetraspanin-like sequence and satisfied the screening criteria. The protein, referred to as IRF-3–dependent NK-activating molecule (INAM), functioned in both the mDC and NK cell to facilitate NK activation. In the mDC, TICAM-1, IFN promoter stimulator 1, and IRF-3, but not IRF-7, were required for mDC-mediated NK activation. INAM was minimally expressed on NK cells, was up-regulated in response to polyI:C, and contributed to mDC–NK reciprocal activation via its cytoplasmic tail, which was crucial for the activation signal in NK cells. Adoptive transfer of INAM-expressing mDCs into mice implanted with NK-sensitive tumors caused NK-mediated tumor regression. We identify a new pathway for mDC–NK contact-mediated NK activation that is governed by a TLR signal-derived membrane molecule.

CORRESPONDENCE
Tsukasa Seya:
seya-tu@pop.med.hokudai.ac.jp

Abbreviations used: BMDC, BM-derived DC; IKK, IκB kinase; INAM, IRF-3–dependent NK-activating molecule; IPS-1, IFN promoter stimulator 1; IRF, IFN regulatory factor; mDC, myeloid DC; PRR, pattern recognition receptor; Rae-1, retinoic acid–inducible gene 1; TICAM-1, toll/IL-1 receptor homology domain–containing adaptor molecule 1; TLR, Toll-like receptor.

Natural killer (NK) cells contribute to innate immune responses by killing virus-infected or malignantly transformed cells and by producing cytokines such as IFN-γ and TNF. NK cell activation is determined by a balance of signals from inhibitory and activating receptors. Because ligands of inhibitory receptors include MHC class I and class I–like molecules, the absence of self-MHC expression leads to NK activation (Cerwenka and Lanier, 2001). Approximately 20 receptors contribute to NK activation (Cerwenka and Lanier, 2001; Vivier et al., 2008). When ligands for activating receptors are sufficiently abundant, activating signals overcome inhibitory signals.

There are two currently accepted models for in vivo NK activation. One is that NK cells usually circulate in a naive state and are activated through interaction directly with ligands for pattern recognition receptors (PRRs) expressed by NK cells or interaction with cells that express PRR ligands (Hornung et al., 2002; Sivori et al., 2004). When pathogens enter the host, innate immune sensors, such as Toll-like receptors (TLRs), RIG-I-like receptors,

T. Ebihara and M. Azuma contributed equally to this paper.
T. Ebihara's present address is Howard Hughes Medical Institute, Washington University School of Medicine, St. Louis, MO 63110.

The Rockefeller University Press $30.00
J. Exp. Med. Vol. 207 No. 12 2675-2687
www.jem.org/cgi/doi/10.1084/jem.20091573

Supplemental Material can be found at:
http://jem.rupress.org/content/suppl/2010/11/04/jem.20091573.DC1.html

Published November 8, 2010

NOD-like receptors, and lectin family proteins, which are PRRs, recognize a variety of microbial patterns (pathogen-associated molecular patterns [PAMPs]; Medzhitov and Janeway, 1997). Mouse NK cells express almost all TLRs (TLR1–3, 4, and 6–9), and some of these are directly activated by pathogens with the help of IL-12, IL-18, IFN-γ, and other cytokines (Newman and Riley, 2007). The other is that naive NK cells tend to be recruited to the draining LNs, where they are primed to be effectors with the help of mature myeloid DCs (mDC) and released into peripheral tissues (Fernandez et al., 1999). In this case, mDCs provide direct activating signals to NK cells through cell–cell contact (Gerosa et al., 2002; Akazawa et al., 2007a; Lucas et al., 2007). mDCs also produce proinflammatory cytokines and IFN-α after recognizing PAMPs (Newman and Riley, 2007). In this mDC-mediated NK activation, however, the molecules and mechanisms in mDC that are dedicated to NK activation in vivo remain to be understood.

In this study, we focused on the molecules that are induced in mDC during maturation by exposure to double-stranded (ds) RNA and the molecules involved in priming NK cells for target killing (Akazawa et al., 2007a). dsRNA of viral origin and the synthetic analogue polyI:C induce NK activation in concert with mDC in vivo and in vitro (Seya and Matsumoto, 2009). PolyI:C is recognized by the cytoplasmic proteins RIG-I/MDA5 and the membrane protein TLR3, both of which are expressed in mDC (Matsumoto and Seya, 2008). Although RIG-I and MDA5 in the cytoplasm deliver a signal to the adaptor protein IFN promoter stimulator 1 (IPS-1; also known as MAVS, VISA, and Cardif) on the outer membrane of the mitochondria (Kawai et al., 2005; Meylan et al., 2005; Seth et al., 2005; Xu et al., 2005), TLR3 in the endosomal membrane recruits the adaptor protein toll/IL-1 receptor homology domain–containing adaptor molecule 1 (TICAM-1)/TRIF (Oshiumi et al., 2003a; Yamamoto et al., 2003a). Both adaptor proteins activate TBK1 and/or IκB kinase (IKK) ε, which phosphorylate IFN regulatory factor (IRF) 3 and IRF-7 to induce type I IFN (Sasai et al., 2006). We previously showed that the TLR3–TICAM-1 pathway in mDC participates in inducing anti-tumor NK cytotoxicity by polyI:C (Akazawa et al., 2007a). mDC matured with polyI:C can enhance NK cytotoxicity through mDC-NK cell–cell contact (Akazawa et al., 2007a). Therefore, we hypothesized that an unidentified protein is up-regulated on the cell surface of mDC through activation of the TLR3–TICAM-1 pathway, and this protein enables mDC to interact with and activate NK cells. This is the first study identifying an IRF-3–dependent NK-activating molecule, which we abbreviated INAM. INAM is a TICAM-1–inducible molecule on the cell surface of BM-derived DCs (BMDCs) that activates NK cells via cell–cell contact. Our data imply that mDCs harbor a pathway for driving NK activation that acts in conjunction with dsRNA and TLR3.

RESULTS

TICAM-1/IRF-3 signal in BMDCs augments NK activation

An in vitro system for evaluating NK activation through BMDC-NK contact was established for this study (Fig. 1 A). A mouse melanoma cell subline B16D8, which was established in our laboratory as a low H-2 expressor (Mukai et al., 1999), was used as an NK target. PolyI:C, WT BMDC, and NK cells were all found to be essential for NK-mediated B16D8 cytolysis in the in vitro assay (Fig. 1 A). PolyI:C-mediated NK activation was at baseline levels in a transwell with a 0.4-μm pore, suggesting the importance of direct BMDC-NK contact for this cytolysis induction (Fig. 1 A). When WT BMDCs were replaced with TICAM-1$^{-/-}$ BMDCs in this system, polyI:C-mediated NK activation was partly abolished (Fig. 1 B; and Fig. S1, A and B). TICAM-1 of BMDC was involved in driving NK activation, and ultimately B16D8 cells were damaged by BMDC-derived NK cells (Fig. 1 B). PolyI:C-mediated NK activation occurred even when WT NK cells were replaced with TICAM-1$^{-/-}$ NK cells (Fig. 1 B), which means that NK activation barely depends on the TICAM-1 pathway in NK cells.

PolyI:C-activated splenic NK cells were i.p. injected into B6 mice to kill B16D8 cells ex vivo, which is consistent with previous studies (McCartney et al., 2009; Miyake et al., 2009), and this polyI:C-mediated NK activation was markedly reduced in IPS-1$^{-/-}$ mice established in our laboratory (Fig. S1 C), suggesting that NK cell activation is induced via not only the TICAM-1 pathway but also the IPS-1 pathway, which was largely comparable with previous studies (McCartney et al., 2009; Miyake et al., 2009). IPS-1 in BMDC was more involved in polyI:C-driven NK cytotoxicity than TICAM-1 but almost equally contributed to NK-dependent IFN-γ induction to TICAM-1 in our setting (Fig. S1 B). In addition, the serum level of IL-12p40 in polyI:C-treated mice was largely dependent on TICAM-1 (Fig. S1 D; Kato et al., 2006; Akazawa et al., 2007a). In the supernatant of polyI:C-stimulated BMDC and the serum samples from polyI:C-treated mice, IL-12p70 was not detected by ELISA (unpublished data). These results suggest that polyI:C activates NK cells largely secondary to mDC maturation, which is sustained by the IPS-1 or TICAM-1 pathway of mDC. Even though NK cells express TLR3, they are only minimally activated by polyI:C alone. Signaling by TICAM-1 in BMDC can augment NK cytotoxicity and IFN-γ production via BMDC/NK contact.

The TICAM-1 pathway activates the transcription factor IRF-3. More precisely, exogenous addition of polyI:C can activate endosomal TLR3 and cytoplasmic RIG-I/MDA5. RIG-I/MDA5 assembles the adaptor IPS-1, which in turn recruits the NAP1–IKK-ε–TBK1 kinase complex and activates both IRF-3 and IRF-7 (Fitzgerald et al., 2003; Yoneyama et al., 2004). For this reason, we examined the role of IRF-3 and IRF-7 in BMDC for activation of NK cells by polyI:C. Activation of IRF-3, but not IRF-7, was required for BMDC to induce NK cytotoxicity (Fig. 1 C). IL-2 (Zanoni et al., 2005), IFN-α (Gerosa et al., 2002), and trans-presenting IL-15 (Lucas et al., 2007) induced by BMDC are reported to be key cytokines for BMDC-mediated NK activation in response to polyI:C. However, even with normal levels of IFN-α production and IL-15 expression (Fig. 1, D and E), TICAM-1$^{-/-}$ BMDCs failed to induce full NK cytotoxicity (Fig. 1 B). In contrast, IRF-7$^{-/-}$ BMDCs, which have impaired IFN-α and IL-15

Published November 8, 2010

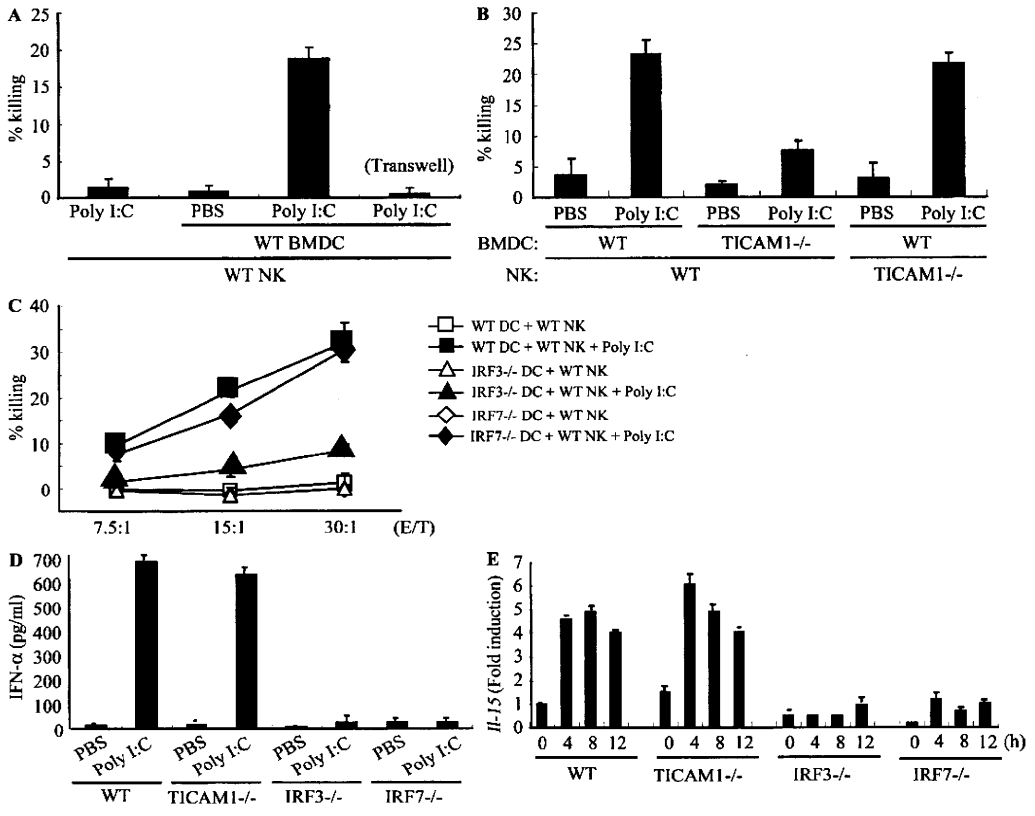

Figure 1. IRF-3 in BMDC controls the capacity to activate NK cells in response to polyI:C. (A and B) WT or TICAM-1$^{-/-}$ NK cells were co-cultured with WT or TICAM-1$^{-/-}$ BMDC in the presence of 10 μg/ml polyI:C for 24 h. NK cytotoxicity against B16D8 was determined by standard ^{51}Cr release assay. E/T = 30. (C) WT NK cells were co-cultured with WT (□, ■), IRF-3$^{-/-}$ (△, ▲), or IRF-7$^{-/-}$ (◇, ◆) BMDC in the presence (■, ▲, ◆) or absence (□, △, ◇) of 10 μg/ml polyI:C for 24 h. NK cytotoxicity against B16D8 was determined by standard ^{51}Cr release assay at the indicated E/T ratio. (D) ELISA of IFN-α in cultures of WT, TICAM-1$^{-/-}$, IRF-3$^{-/-}$, and IRF-7$^{-/-}$ BMDC treated with 10 μg/ml polyI:C for 24 h. (E) Quantitative RT-PCR for IL-15 expression in BMDC stimulated with 10 μg/ml polyI:C. All data are means ± SD of duplicate or triplicate samples from one experiment that is representative of three.

expression, fully activated NK cells (Fig. 1, C–E). Hence, in BDMCs, the TICAM-1–IRF-3 pathway, rather than other cytokines, appears to induce cell surface molecules that mediate BMDC/NK contact and evoke NK cytotoxicity.

Identification of INAM

To identify the NK-activating cell surface molecule on BMDC, we performed microarray analysis on polyI:C-stimulated BMDC prepared from TICAM-1$^{-/-}$ and WT mice. The results yielded nine TICAM-1–inducible molecules with transmembrane motifs (Table S1). Six were induced in an IRF-3–dependent manner, whereas three were still induced in IRF-3$^{-/-}$ BMDC. The NK-activating ability of the products of these genes was investigated by introduction of lentivirus expression vector into IRF-3$^{-/-}$ BMDC. BMDCs with the transduced genes were co-cultured with WT NK cells and polyI:C, and the NK-activating ability was evaluated by determining IFN-γ in the 24-h co-culture. NK cells, but not the gene-transduced BMDCs, produced IFN-γ in the presence of polyI:C. Finally, we identified a tetraspanin-like molecule that satisfied our evaluation criteria (IFN-γ and cytotoxicity) on the mDC-NK activation and named this molecule INAM. INAM clearly differed from other tetraspanins like CD9, CD63, CD81, CD82, and CD151 in the predicted structure. Mouse INAM is a 40–55-kD protein with one N-glycosylation site and possesses four transmembrane motifs (Fig. 2, A and B). Western blotting analysis of INAM-transfected cells under nonreducing conditions showed no evidence of multimers (Fig. 2 B). The N-terminal and C-terminal regions of INAM are in the cytoplasm because anti-Flag antibody did not detect C-terminal Flag-tagged INAM until cells were permeabilized (unpublished data).

Alignment of the predicted amino acid sequence of mouse INAM with that of the human orthologue revealed that the two INAMs shared a 71.7% amino acid identity. INAM is also called FAM26F (Table S1) and is in the FAM26 gene family (Bertram et al., 2008; Dreses-Werringloer et al., 2008). Sequence database searches identified six mouse INAM paralogs. Although FAM26A/CALHM3, FAM26B/CALHM2, and FAM26C/CALHM1 are located on chromosome 19, FAM26D, FAM26E, and FAM26F/INAM are on chromosome 10. Only INAM was inducible with TLR agonists (unpublished data). All FAM26 family proteins have three or four transmembrane motifs predicted by the TMHMM Server (version 2.0). Human CALHM1 has a conserved region (Q/R/N site)

Published November 8, 2010

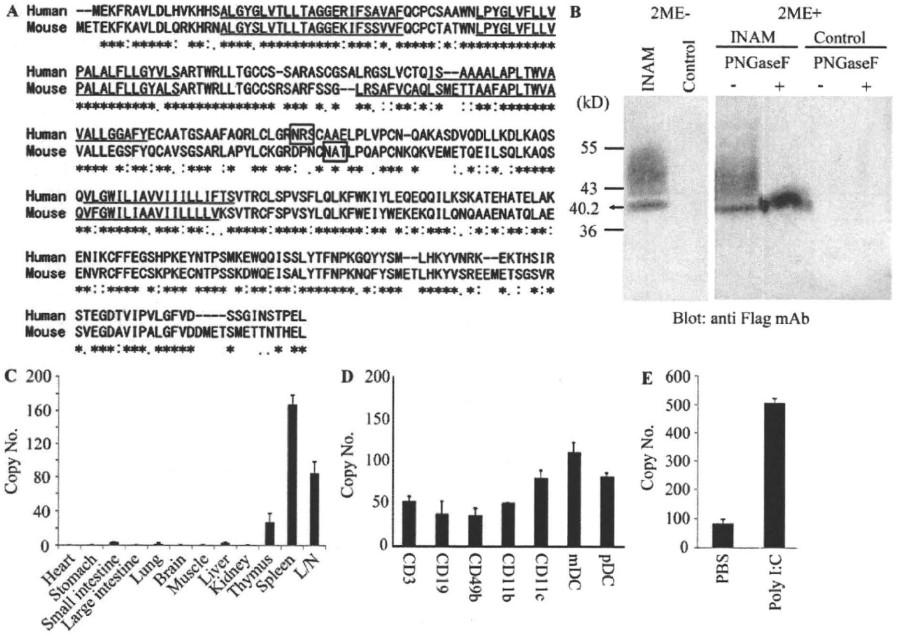

Figure 2. Sequence alignment of INAM and expression of INAM. (A) Sequence alignment of human and mouse INAM. Asterisks, identical residues; double dots, conserved substitutions; single dots, semiconserved substitutions; box, N-glycosylation site; underline, transmembrane motif. (B) Immunoblot analysis of lysates of 293FT cells transfected with plasmid encoding Flag-tagged INAM. PNGase, *N*-glycosidase. 2ME, 2-mercaptoethanol. (C and D) Quantitative RT-PCR for INAM expression in mouse tissue (C) and spleen cells (D). $CD3^+$, $CD19^+$, $DX5^+$, $CD11b^+$, $CD11c^+$, mDC ($CD11c^+PDCA1^+$), and plasmacytoid DC (pDC; $CD11c^+PDCA1^+$) cells were isolated from splenocytes by cell sorting. Data are expressed as copy number per 10^4 copies of HPRT. Data shown are means ± SD of triplicate samples from one experiment that is representative of three. (E) Augmented INAM expression in LN cells after polyI:C stimulation. WT mice were i.p. injected with 100 µg polyI:C or control buffer. After 24 h, inguinal, axillary, and mesenteric LN were harvested and RNA was extracted from the LN cells. The levels of the INAM mRNA were measured by real-time PCR. The results were confirmed in two additional experiments. Data represent mean ± SD.

with ion channel properties at the C-terminal end of the second transmembrane motif that controls cytoplasmic Ca^{2+} levels (Dreses-Werringloer et al., 2008). However, the Q/R/N site was not found in INAM. CALHM1, 2, and 3 are highly expressed in brain. Quantitative RT-PCR revealed that INAM expression was high in spleen and LNs but low in thymus, liver, lung, and small intestine (Fig. 2 C), although expression of the other two FAM26 family members from chromosome 10 was highest in brain (not depicted). All splenocytes examined ($CD3^+$, $CD19^+$, $DX5^+$, $CD11b^+$, $CD11c^+$, mDCs [$CD11c^+$ $PDCA1^-$], and plasmacytoid DCs [$CD11c^-PDCA1^+$]) expressed INAM to some levels (Fig. 2 D). The INAM expression was inducible by polyI:C in LN cells (Fig. 2 E); the induction levels were more prominent in myeloid cells than in lymphocytes in the LNs (Fig. S2 A). $NKp46^+$ and $DX5^+$ NK cells also expressed INAM with low levels and the levels were mildly increased by polyI:C stimulation (Fig. S2 A and not depicted). Notably, only $CD45^+$ cells expressed INAM, which excludes the participation of contaminating stromal cells in the INAM up-regulation (Fig. S2 B).

BMDC INAM activates NK cells

WT and IRF-$7^{-/-}$ BMDCs induced high NK cytotoxicity in response to polyI:C, whereas TICAM-$1^{-/-}$, IPS-$1^{-/-}$, and IRF-$3^{-/-}$ BMDC showed less NK activation (Fig. 1, B and C; and Fig. S1). INAM expression profile by polyI:C stimulation was then examined using WT, IRF-$3^{-/-}$, IRF-$7^{-/-}$, and TICAM-$1^{-/-}$ BMDCs. Stimulation with polyI:C induced INAM at normal levels in IRF-$7^{-/-}$ BMDC but at decreased levels in IRF-$3^{-/-}$ and TICAM-$1^{-/-}$ BMDC (Fig. 3 A). The expression profiles of INAM in polyI:C-stimulated BMDC were in parallel with those inducing NK activation. BMDCs express a variety of TLRs (Iwasaki and Medzhitov, 2004), but other TLR ligands, Pam_3CSK_4 for TLR1/2, Malp2 for TLR2/6, and CpG for TLR9, barely induced INAM on BMDC. High induction of INAM was observed in BMDC stimulated with LPS as well as polyI:C (Fig. 3 B), both of which can activate TICAM-1 to induce IRF-3 and IFN-α activation (Fitzgerald et al., 2003; Oshiumi et al., 2003a,b; Yamamoto et al., 2003a,b). Because INAM is an IFN-inducible gene (Fig. 3 B), INAM induction may be amplified by type I IFNs.

We next examined whether INAM was localized to the cell surface membrane in BMDC. Immunofluorescence analysis showed Flag-tagged INAM on the cell surface of BMDC. Plasma membrane expression of INAM was also confirmed by cell surface biotinylation (Fig. S3). Although the lentivirus inefficiently infected BMDC, GFP expression levels were similar in cells with control virus and those with INAM-expressing virus (Fig. 3 C). Transduction efficiency and expression from the lentivirus vector were adjusted using GFP expression (not depicted), and surface INAM expression was further confirmed with BMDC, NK cells, and INAM-expressing BaF3 (INAM/BaF3) cells, in some cases using polyclonal antibody (Ab) against INAM (Fig. S4).

We then examined whether overexpressing INAM resulted in signaling that directed BMDC maturation and production of cytokines, including IFN-α and IL-12p40, which are reported to enhance NK activity (Gerosa et al., 2002; Sivori et al., 2004; Lucas et al., 2007). The status of INAM-transduced BMDC was assessed by CD86 expression and cytokine production, and no significant differences in these maturation markers were seen in BMDC overexpressing INAM (Fig. S5). In the same setting, no IL-12p70 was

Published November 8, 2010

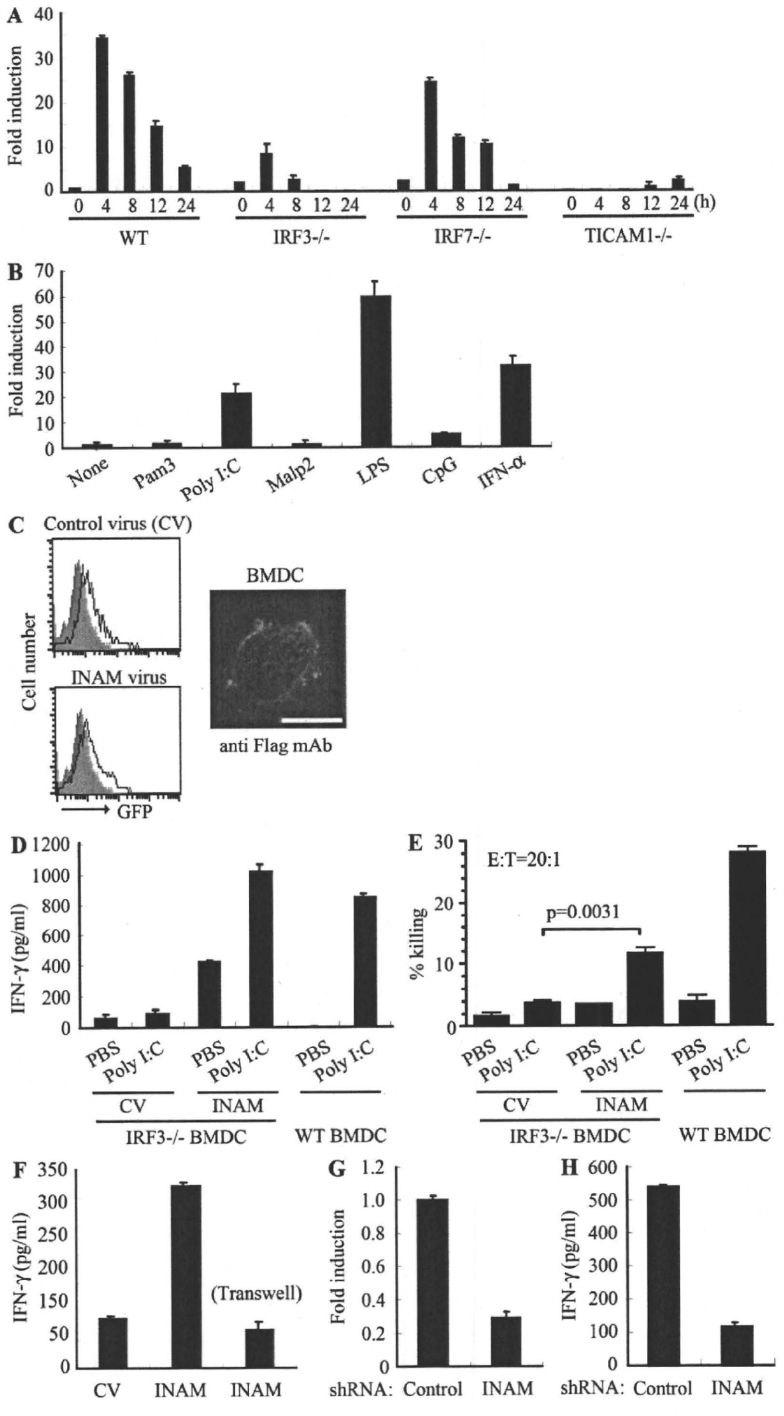

Figure 3. INAM in BMDC participates in DC-mediated NK activation. (A) Quantitative RT-PCR for INAM expression in WT, TICAM-1$^{-/-}$, IRF-3$^{-/-}$, and IRF-7$^{-/-}$ BMDC stimulated with 10 µg/ml polyI:C. (B) Quantitative RT-PCR for INAM expression in WT BMDC stimulated by 100 ng/ml LPS, 10 µg/ml polyI:C, 1 µg/ml Pam3, 100 nM Malp-2, 10 µg/ml CpG, and 2,000 IU/ml IFN-α for 4 h. (C) BMDCs were transduced with Flag-tagged INAM-expressing lentivirus or control lentivirus. GFP expression in the BMDC was determined by flow cytometry, and subcellular localization of INAM was examined by immunofluorescence assay using anti-Flag mAb. Shaded peak, noninfected control; Blank peak, infected BMDC. Bar, 10 µm. (D) ELISA of IFN-γ induced by WT NK cells co-cultured with WT BMDC or IRF-3$^{-/-}$ BMDC transfected with control lentivirus (CV) or INAM-expressing lentivirus (INAM) with/without 10 µg/ml polyI:C. (E) Cytotoxicity against B16D8 by NK cells co-cultured with BMDC transfected with control or INAM-expressing lentivirus with/without 10 µg/ml polyI:C for 24 h. (F) ELISA of IFN-γ induced by WT NK cells co-cultured with IRF-3$^{-/-}$ BMDC transfected with control lentivirus (CV) or INAM-expressing lentivirus (INAM) with 10 µg/ml polyI:C. In some experiments, a transwell was inserted between the INAM-transduced BMDC and NK cells to separate the cells. (G) Quantitative RT-PCR for expression of INAM in BMDC transduced with INAM-shRNA (INAM) or scrambled shRNA (control) and cultured for 48 h. (H) IFN-γ production by WT NK cells determined using ELISA after coculturing with control or the shRNA transfected-BMDC (INAM) and 10 µg/ml polyI:C for 24 h. All data shown are means ± SD of triplicate samples from one experiment that is representative of three.

detected by ELISA (unpublished data). In addition, polyI:C-mediated NK activation occurred in BMDC expressing an INAM mutant lacking the cytoplasmic C-terminal region (193–327 aa; Fig. 4, A and B), excluding the participation of the cytoplasmic region in BMDC maturation signaling.

To investigate whether INAM could reconstitute NK-activating ability in IRF-3$^{-/-}$ BMDC, we transduced INAM into IRF-3$^{-/-}$ BMDC and incubated BMDC with NK cells. Overexpression of INAM in IRF-3$^{-/-}$ BMDC induced NK IFN-γ production and NK cytotoxicity against B16D8, and this NK activation was further enhanced by the addition of polyI:C (Fig. 3, D and E). Thus, polyI:C may also work for NK activation. Direct cell–cell contact with NK cells was required for INAM in IRF-3$^{-/-}$ BMDC to function on enhancing NK activity (Fig. 3 F).

We further confirmed this issue using WT BMDC by shRNA gene silencing. We silenced the INAM gene in BMDC using the lentiviral vector pLenti-dest-IRES-hrGFP and monitored expression by GFP. Because transfection efficiency was relatively high in this case compared with that shown in Fig. 3 C, the expression level of INAM had decreased by ~75% in WT BMDC compared with the nonsilenced control (Fig. 3 G and Fig. S6 A). Although the level of the endogenous INAM protein was not very high, we confirmed that INAM protein was also decreased by shRNA with immunoblotting using anti-INAM pAb (Fig. S7 A). PolyI:C response of BMDC-inducible cytokines tested was not altered by INAM silencing in BMDC (Fig. S6 B). Yet this INAM RNA interference caused a significant decrease in NK cell IFN-γ production after co-culture of the INAM knockdown BMDCs and WT NK cells with polyI:C (Fig. 3 H). Collectively, these results indicate that INAM is downstream of IRF-3 in BMDC and is involved in the activation of NK cells by BMDC.

Published November 8, 2010

Using an INAM-expressing stable BaF3 cell line (INAM/BaF3), we tested the possibility that INAM is an activating ligand for NK cells. As a positive control, we produced a stable BaF3 cell line expressing Rae-1α (Fig. 5 A) which is a ligand for the NK-activating receptor NKG2D (Cerwenka et al., 2000). Although Rae-1α/BaF3 cells were easily damaged by IL-2–activated NK cells, INAM/BaF3 cells were not (Fig. 5 B). In this context, addition of IRF-3$^{-/-}$ BMDC to this culture with BaF3 and NK cells led to slight augmentation of IFN-γ induction irrespective of the presence of INAM on BaF3 cells (Fig. 5 C), and β2-microglobulin$^{-/-}$ BMDC barely affected the IFN-γ level (not depicted). These results suggest that an INAM-containing molecular matrix, rather than INAM alone, acts toward NK cells. Alternatively, INAM may selectively function with specific mDC molecules to activate NK cells.

INAM on NK cells is required for efficient NK activation

mDCs were previously shown to be required for efficient NK activation in vivo and in vitro (Akazawa et al., 2007a). We found that INAM was minimally present in BMDCs and NK cells and that polyI:C acts on both (Figs. S2 A; and Fig 3, D and E). Tetraspanin-like molecules tend to work as scaffolds for heteromolecular complexes that contain molecules functioning in a cis- or trans-adhesion manner to exert intercellular or extracellular functions. Thus, the function of INAM may not be confined to mDC, so we studied the function of INAM on NK cells. In NK cells, INAM was also inducible by polyI:C (Fig. 6 A and Fig. S2 A), and the induction of INAM was abrogated completely in IRF-3$^{-/-}$ NK cells and moderately in TICAM1$^{-/-}$ NK cells (Fig. 6 B). This suggests that polyI:C also acts on NK cells and induces INAM through IPS-1/IRF-3 activation when NK cells are co-cultured with BMDC and polyI:C.

To investigate whether INAM induced in NK cells is associated with BMDC-mediated NK activation, we performed the following experiments (Fig. 6 C). INAM-transduced IRF-3$^{-/-}$ BMDCs were incubated with polyI:C for 4 h, and then the aliquot was mixed with WT NK cells in the presence of polyI:C (Fig. 6 C, left two lanes). A moderate increase of IFN-γ was observed as in Fig. 3 D. In the remainder,

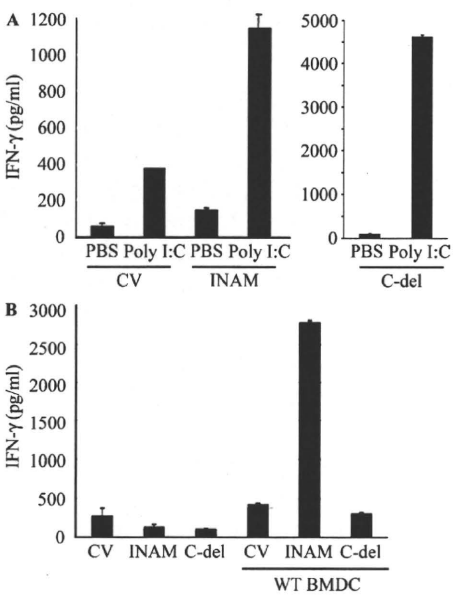

Figure 4. Role of the cytoplasmic tail of INAM. (A) The C-terminal region of INAM was not required for BMDC-mediated NK activation. ELISA of IFN-γ by WT NK cells co-cultured with IRF-3$^{-/-}$ BMDCs transfected with control lentivirus (CV) or a lentivirus expressing intact INAM or a mutant INAM lacking the C-terminus (C-del INAM) with/without 10 μg/ml polyI:C. Data shown are means ± SD of triplicate samples from one experiment representative of three. (B) The cytoplasmic tail of INAM is indispensable for NK IFN-γ induction. INAM or C-del INAM (A) was expressed on IRF-3$^{-/-}$ NK cells. The INAM (or C-del INAM)-expressing IRF-3$^{-/-}$ NK cells were incubated with or without WT BMDC for 24 h. IFN-γ levels in the supernatants were determined by ELISA. One representative result out of several similar experiments is shown. Data represent mean ± SD.

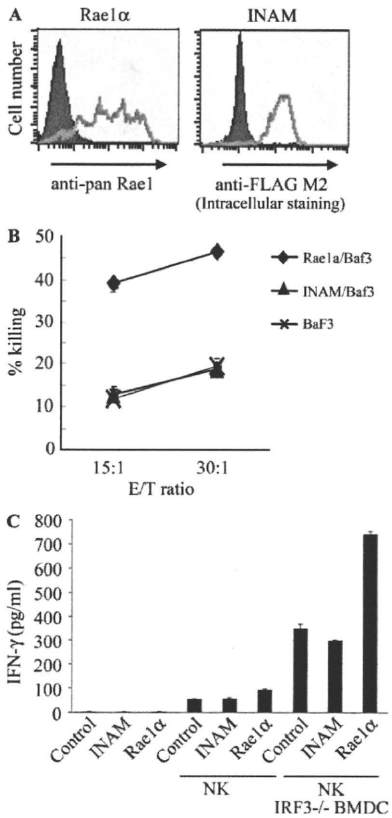

Figure 5. INAM is not an NK-activating ligand. (A) Flow cytometry for Rae-1 and Flag-tagged INAM in stable BaF3 lines. Shaded peak, untransfected control BaF3 staining with anti-pan-Rae-1 Ab or anti-Flag M2 antibody; open peak, stable Rae-1α/BaF3 or stable Flag-tagged INAM/BaF3 staining with anti-pan-Rae-1 antibody or anti-Flag M2 antibody. (B) Cytotoxicity against control BaF3, Rae-1α/BaF3, and INAM/BaF3 by NK cells treated with 1,000 IU/ml IL-2 for 3 d. Data shown are means ± SD of triplicate samples from one experiment representative of three. (C) NK activation is augmented by coexistent BMDC irrespective of INAM expression. NK cells were cultured with 1,000 IU/ml IL-2 for 3 d. 2 × 10^5 NK cells, 10^5 BaF3 cells, and 10^5 IRF-3$^{-/-}$ BMDCs were co-cultured in 200 μl/well and IFN-γ in the supernatants were measured by ELISA. Data show one of two similar experimental results. Data represent mean ± SD.

Published November 8, 2010

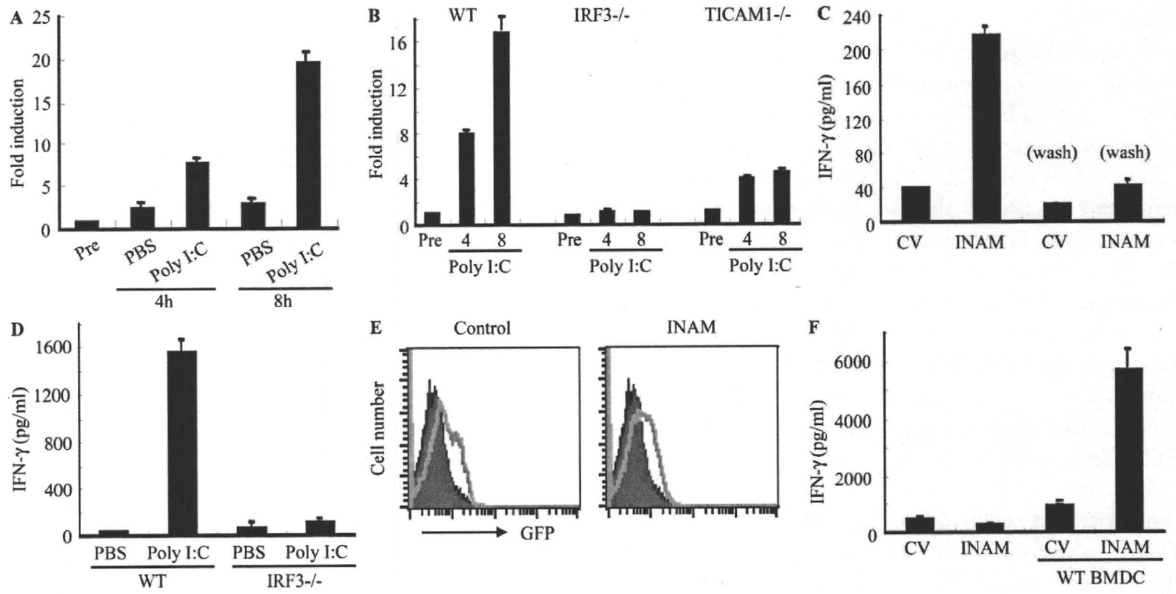

Figure 6. INAM on NK cells contributes to efficient NK activation mediated by mDC. (A and B) Quantitative RT-PCR for INAM expression in WT, TICAM1$^{-/-}$, or IRF-3$^{-/-}$ NK cells stimulated with 50 µg/ml polyI:C. Data shown are means of duplicate or triplicate samples from one experiment that is representative of three. (C) IRF-3$^{-/-}$ BMDCs were transfected with control lentivirus (CV) or INAM-expressing lentivirus (INAM) before treatment with 10 µg/ml polyI:C for 4 h. BMDCs in some wells were washed to remove polyI:C before WT NK cells were added (Wash). IFN-γ production by NK cells was determined by ELISA after 24 h of culture. Data show one of two similar experimental results. (D) ELISA of IFN-γ in co-culture of WT or IRF-3$^{-/-}$ NK cells and WT BMDC with/without 10 µg/ml polyI:C. (E and F) NK cells were transfected with control lentivirus or INAM-expressing lentivirus and cultured with 500 IU/ml IL-2 for 3 d. After determining transfection efficiency by GFP intensity using flow cytometry, cells were cultured with/without BMDC for 24 h and IFN-γ production in the supernatant determined by ELISA. Shaded peak, noninfected control; open peak, infected BMDC. All data are means ± SD of triplicate samples from one experiment that is representative of three.

we washed polyI:C out and cultured the cells with WT NK cells (Fig. 6 C, right two lanes). Under these conditions, in which polyI:C acted not on NK cells but only on BMDC, little NK activation was observed (Fig. 6 C). Furthermore, IRF-3$^{-/-}$ NK cells produced little IFN-γ when co-cultured with WT BMDC and polyI:C (Fig. 6 D). INAM-overexpressing IRF-3$^{-/-}$ BMDC required IRF-3 in NK cells for efficient BMDC-mediated production of IFN-γ from NK cells (Fig. 6 D). We next transduced INAM into IRF-3$^{-/-}$ NK cells using a lentivirus (INAM/pLenti-IRES-hrGFP) to reconstitute NK IFN-γ–producing activity. After many trials with various setting conditions, we found that ~15% of the DX5^{+} NK cell population was both GFP-positive and stained with anti-FLAG mAb when treated with high doses of INAM-expressing lentivirus vector (Fig. S7 B). When IRF-3$^{-/-}$ NK cells were infected with smaller amounts of INAM-expressing lentiviral vector and cultured for 3 d with high concentrations of IL-2 (500 IU/ml), slight but significant GFP expression was confirmed by FACS (Fig. 6 E). Then, the INAM-transduced IRF-3$^{-/-}$ NK cells were co-cultured with WT BMDC. The IRF-3$^{-/-}$ NK cells with INAM expression secreted IFN-γ at significantly higher levels than controls in the presence of WT BMDC (Fig. 6 F). These data indicate that INAM is induced by polyI:C through IRF-3 activation, not only in BMDCs but also in NK cells, and that INAM on NK cells synergistically works with INAM on BMDC for efficient NK cell activation. Both INAMs on BMDC and NK cells are essential for BMDC-mediated NK activation.

We next checked the function of the C-terminal stretch of INAM in NK activation. Although intact INAM works in NK cells to produce IFN-γ in response to BMDC (Fig. 6 F), introduction of C-del INAM into IRF-3$^{-/-}$ NK cells did not result in high induction of IFN-γ in response to BMDC (Fig. 4 C). Thus, INAM participates in NK activation through its cytoplasmic regions, which has no significant role in BMDC for NK activation.

Anti-tumor NK activation via INAM-expressing BMDCs in vivo

mDC-mediated NK activation induces anti-tumor NK cells, which cause regression of NK-sensitive tumors (Kalinski et al., 2005; Akazawa et al., 2007a). We tested the in vivo function of INAM-expressing BMDC using B16D8 tumor-bearing mice. BMDCs were used 24 h after transfection with either INAM/pLenti-IRES-hrGFP or control pLenti-IRES-hrGFP and injected twice a week s.c. around a preexisting tumor in tumor-implanted mice, beginning 11–13 d after tumor challenge. INAM-expressing BMDC significantly retarded tumor growth (Fig. 7 A). Tumor retardation was abrogated by depletion of NK1.1-positive cells (Fig. 7 B). Thus, INAM expression on BMDC contributed to anti-tumor NK activation in vivo.

When the control or INAM-expressing IRF-3$^{-/-}$ BMDCs were co-cultured with WT NK cells in vitro, there was no induction of the mRNA of TRAIL and granzyme B in

Published November 8, 2010

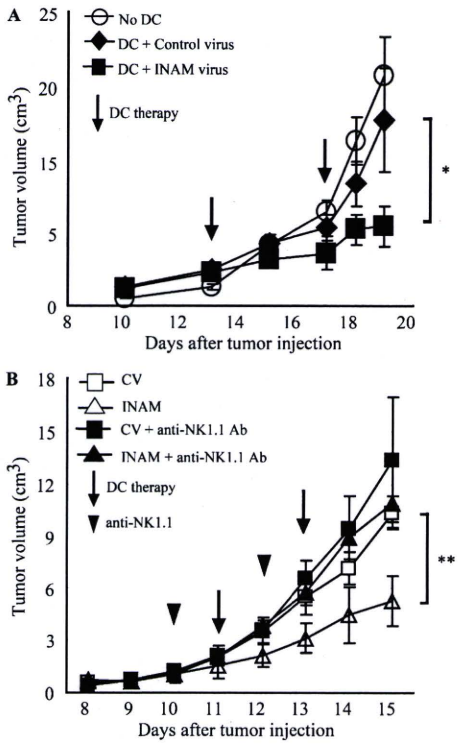

Figure 7. INAM on BMDC retarded B16D8 tumor growth in an NK-dependent manner. (A) Tumor volume after DC therapy using BMDC expressing INAM. B16D8 cells were s.c. injected into C57BL/6 mice and, 11–13 d later, medium only (○) or BMDC (10^6/mouse) transfected with control lentivirus (◆) or those with INAM-expressing lentivirus (■) were administered s.c. near the tumor at the time indicated by the open arrow. *, P = 0.043. Data represent mean ± SD. (B) Abrogation of INAM-dependent tumor regression by administration of NK1.1 Ab. For depletion of NK cells, antiNK1.1 mAb was injected i.p. 1 d before treatment of BMDC (arrowheads). Tumor volume in every mouse group was sequentially monitored. Data represent mean ± SD (n = 3) and are representative of two experiments. Statistical analyses were made with the Student's t test. **, P = 0.017.

NK cells (Fig. 8 A). TRAIL and granzyme B were induced in NK cells by the addition of polyI:C to the mixture, and INAM expression in BMDC up-regulated mRNA levels of TRAIL and granzyme B (Fig. 8 A). In vivo administration studies were performed with polyI:C-treated WT BMDC or INAM-expressing IRF-$3^{-/-}$ BMDC to test their ability to up-regulate the mRNA levels of TRAIL and granzyme B in NK cells in draining LN (Fig. 8 B). INAM-expressing IRF-$3^{-/-}$ BMDC showed comparable abilities to up-regulate the killing effectors with polyI:C-treated BMDC (Fig. 8 B). Collectively, INAM has therapeutic potential for NK-sensitive tumors by activating NK cells.

DISCUSSION

Previous studies demonstrated that mDC–NK interaction leads to direct NK activation and damages NK target cells in vitro (Gerosa et al., 2002; Sivori et al., 2004; Akazawa et al., 2007a; Lucas et al., 2007). In addition, mDCs initiate NK cell–mediated innate anti-tumor immune responses in vivo (Kalinski et al., 2005; Akazawa et al., 2007a,b). Systemic administration of polyI:C unequivocally results in activation of peripheral NK cells (Lee et al., 1990; Sivori et al., 2004; Akazawa et al., 2007a). Although the molecular mechanism by which mDCs prime NK cells was still unclear, the TICAM-1 pathway and IPS-1 pathway have been reported to participate in polyI:C-mediated mDC maturation that drives NK activation (Akazawa et al., 2007a; McCartney et al., 2009; Miyake et al., 2009). We have shown in an earlier study that mDCs disrupted in the TLR3–TICAM-1 pathway abrogate NK cell activation (Akazawa et al., 2007a,b). In TICAM-$1^{-/-}$ mice, NK-sensitive implant tumors grew as well as those in WT mice depleted of NK cells (Akazawa et al., 2007a). mDCs gain high anti-tumor potential against B16D8 implant tumors through lentiviral transfer of TICAM-1, which is attributable to NK activation (Akazawa et al., 2007a). We further showed that TICAM-1 is a critical molecule for mDC to induce NK cell IFN-γ, as well as IPS-1, and participates in driving NK cytotoxicity to a lesser extent than IPS-1. In this paper, we clarified a molecular mechanism by which mDCs immediately promote NK cell functions in vitro and in vivo.

Our findings showed that IRF-3 is the transcription factor that is downstream of TICAM-1 responsible for maturing mDC to an NK-activating phenotype. We discovered that INAM, a membrane-associated protein, is up-regulated on the surface of mDC by polyI:C stimulation and activates NK cells via cell–cell contact. Furthermore, we found that NK cells also express INAM on their cell surface after polyI:C stimulation. mDC–NK activation by polyI:C can be reproduced with INAM-transduced mDC and NK cells, and adoptive transfer experiments show that INAM-overexpressing mDC may have therapeutic potential against MHC-low melanoma cells in an NK-dependent manner. These functional properties of INAM-expressing mDC fit the model of mDC priming NK activation. Ultimately, INAM appears to be the key molecule in the previously reported mechanism of mDC–NK contact activation.

After the submission of this manuscript, two papers were published that found that the MDA5–IPS-1 pathway in mDC is more important for driving NK activation, particularly in vivo (McCartney et al., 2009; Miyake et al., 2009). Our data also support this point using the IPS-$1^{-/-}$ mice we established (Fig. S1). However, polyI:C, when i.v. administered into mice, may stimulate other systemic cells in addition to $CD8^+$ mDC in vivo (McCartney et al., 2009). The difference among the two (McCartney et al., 2009; Miyake et al., 2009) and this study may be attributed to the setting conditions, which are not always comparable. Moreover, it remains to be settled whether TICAM-1 and IPS-1 take the same INAM complex as a common NK activator in mature mDC and whether TLR3 (or MDA5) KO is equivalent to TICAM-1 (or IPS-1) KO in the mDC–NK activation model. In either case, however, up-regulation of mDC TICAM-1–mediated NK cytotoxicity and IFN-γ induction are feasible with polyI:C under three different conditions (Akazawa et al., 2007a; McCartney et al., 2009; Miyake et al., 2009). Our results infer that INAM participates in at least these mDC–NK interactions.

Published November 8, 2010

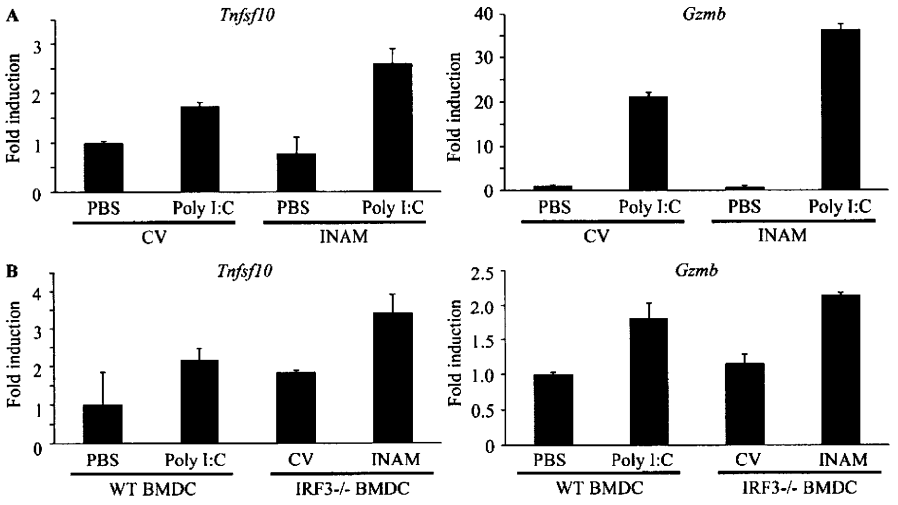

Figure 8. INAM-mediated induction of TRAIL and granzyme B in BMDC. (A) In vitro induction of TRAIL (Tnfsf10) and granzyme B (Gzmb) mRNA by INAM-expressing BMDC. BMDCs (IRF-3$^{-/-}$) were infected with INAM-expressing virus or CV as in Fig. S4. After 24 h, the BMDCs (IRF-3$^{-/-}$) were incubated with WT NK cells at DC/NK = 1:2. 8 h later, DX5^{+} cells were collected by FACS sorting and their RNA was extracted to determine the mRNA levels of the indicated genes. A representative result of three similar experiments are shown. (B) In vivo induction of TRAIL and granzyme B mRNA by INAM-expressing BMDC. WT BMDCs were stimulated with 10 µg/ml polyI:C or medium only. IRF-3$^{-/-}$ BMDCs were infected with CV or INAM-expressing vector. These BMDCs were allowed to stand for 24 h and then 5 × 10^{5} cells were injected into footpads of WT mice. After 48 h, DX5^{+} cells were collected from the inguinal LN by FACS sorting. RNA of the cells was extracted and the levels of the indicated mRNA were determined by real time PCR. Data show one of two experiments with similar results. Data in A and B represent mean ± SD.

PolyI:C activates IRF-3 through the two pathways involving the adaptors IPS-1 and TICAM-1 (Yoneyama et al., 2004; Kato et al., 2006; Matsumoto and Seya, 2008). The two pathways share the complex of IRF-3–activating kinase, NAP1, IKK-ε, and TBK1 that is downstream of adaptors (Sasai et al., 2006). Nevertheless, these pathways are capable of inducing several genes unique to each adaptor. Although IFN-α production by in vivo administration of polyI:C is largely dependent on the IPS-1 pathway, IL-12p40 is mainly produced by the TICAM-1 pathway (Kato et al., 2006). Therefore, it is not surprising that INAM induction is predominant in the TICAM-1 pathway in polyI:C-stimulated BMDC (Fig. 3 A). What happens in IRF-7$^{-/-}$ BMDCs in terms of INAM induction and what mechanism sustains BMDC IPS-1–mediated or MyD88-mediated activation of NK cells (Azuma et al., 2010) will be issues to be elucidated in the future.

Although IRF-3–regulated cell surface INAMs are required for efficient interaction between BMDC and NK cells, the mechanism by which forced expression of INAM causes signaling for BMDC maturation is still unknown. Although the NK-activating capacity of BMDCs is usually linked to their maturation, neither cytokines in NK activation, including IFN-α and IL-12p70, nor costimulators, such as CD40 and CD86, were specifically induced in mDC by INAM expression (Fig. S5). INAM has a C-terminal cytoplasmic stretch (Fig. 4 A), and we tested the function of this region by a deletion mutant (C-del INAM). This region in BMDC barely participates in driving NK activation because no decrease of IFN-γ induction by NK cells was observed with IRF-3$^{-/-}$ BMDC supplemented with C-del INAM compared with control INAM. Thus far, no significant signal alteration has been detected in BMDC supplemented with INAM by lentivirus.

In contrast, INAM-transduced IRF-3$^{-/-}$ NK cells produced IFN-γ in concert with BMDCs like WT NK cells (Fig. 6 F). So far we have no evidence suggesting that this kind of INAM overexpression is actually occurring in vivo. However, introduction of C-del INAM into IRF-3$^{-/-}$ NK cells did not result in high induction of IFN-γ in response to BMDC (Fig. 4 C). Together with the data on INAM expression in BMDC, this infers that the INAM cytoplasmic region signals for NK activation in NK cells. The one-way role of the cytoplasmic tail in NK activation will be an issue for further analysis.

In this study, IL-15 was found to be up-regulated by polyI:C in BMDC. The remaining NK activity in the resting population of NK cells co-cultured with TICAM-1$^{-/-}$ BMDC and polyI:C (Fig. 1 B) suggests that IL-15 has some effect in our system, and other studies suggest this as well (Ohteki et al., 2006; Brilot et al., 2007; Lucas et al., 2007; Huntington et al., 2009). However, we did not observe decreased IL-15 expression in the TICAM-1$^{-/-}$ BMDC that could not activate NK cells (Fig. 1 E). Several molecules, such as B7-H6/NKp30 (Brandt et al., 2009), CD48/2B4 (Kubin et al., 1999), and NKG2D ligands/NKG2D (Cerwenka et al., 2000), have been identified as ligand/receptor molecules in mDC–NK reciprocal activation by in vitro co-culture. In in vitro co-culture systems (Fig. S1), the IPS-1 pathway in BMDC has a pivotal role in not only type I IFN but also IL-15 induction. INAM identified in this paper serves a unique function in the in vivo induction of NK activation and may offer a tool to investigate the reported mDC-mediated NK activation.

Rae-1 was reported as a molecule with MHC-like structure (Zou et al., 1996) and later identified as a mouse NKG2D ligand (Cerwenka et al., 2000). Although Rae-1 is a GPI-anchored protein with no cytoplasmic sequences (Nomura et al., 1996), it can act as an NK-activating ligand (Cerwenka et al., 2000, 2001; Masuda et al., 2002). Mouse BaF3 cells become NK-sensitive after forced expression of Rae-1α (Masuda et al., 2002). Actually, mouse macrophages induce Rae-1 expression in response to TLR stimuli (Hamerman et al., 2004). In contrast,

Published November 8, 2010

INAM-expressing stable BaF3 cell lines (INAM/BaF3) did not reveal a function as an NK cell–activating ligand. NK cell cytotoxicity is directed against Rae-1α/BaF3 cells but not against INAM/BaF3 cells (Fig. 5). Therefore, INAM does not represent a typical NK cell–activating ligand. For NK activation, INAM on BMDC appears to require other molecules that are expressed in BMDC but not in BaF3.

INAM has four transmembrane regions, similar to the cell adhesion tetraspanins, which may support cell–cell contact (Levy and Shoham, 2005). Tetraspanins provide a scaffold that facilitates complex formation with associated proteins. INAM on BMDC and NK cells may use cell–cell interaction to assemble in a synaptic formation to activate NK cells. Because the protein constituents of the tetraspanin complexes are cell specific, we are interested in finding partners for INAM that might participate in efficient BMDC–NK interaction. TLR-inducible cell–cell contact may occur through INAM in an immune cell–specific manner. Gene disruption of this INAM will facilitate clarifying this issue. The identification of INAM defines a novel pathway in mDC–NK reciprocal interaction. This study will lead to further research on the molecules that form complexes on BMDC and NK cells to facilitate BMDC–NK interaction.

MATERIALS AND METHODS

Mice. All mice were backcrossed with C57BL/6 mice more then seven times before use. TICAM-1$^{-/-}$ (Akazawa et al., 2007a) and IPS-1$^{-/-}$ mice were generated in our laboratory. IRF-3$^{-/-}$ (Sato et al., 2000) and IRF-7$^{-/-}$ mice (Honda et al., 2005) were provided by T. Taniguchi (University of Tokyo, Tokyo, Japan). All mice were maintained under specific pathogen-free conditions in the animal facility of the Hokkaido University Graduate School of Medicine. Animal experiments protocols and guidelines were approved by the Animal Safety Center, Hokkaido University, Japan.

Cells. The B16D8 cell line was established in our laboratory as a subline of B16 melanoma (Tanaka et al., 1988). This subline was characterized by its low or virtually no metastatic properties when injected s.c. into syngeneic C57BL/6 mice. B16D8 was cultured in RPMI 1640/10% FCS. The mouse B cell line BaF3 was obtained from American Type Culture Collection and cultured in RPMI 1640/10% FCS/2 μM 2ME/5 ng/ml IL-3. Mouse NK cells (DX5$^+$ cell) were positively isolated with MACS Beads (Miltenyi Biotec). Mouse BMDCs were prepared as previously reported (Akazawa et al., 2007a).

For purification of cells from spleen or LN, these tissues were treated with 400 IU MandleU/ml collagenase D (Roche) at 37°C for 25 min in HBSS (Sigma-Aldrich). Then EDTA was added, and the cell suspension was incubated for an additional 5 min at 37°C. After removal of RBC with ACK lysis buffer, splenocytes and LN cells were stained with CD45-FITC, CD3ε-PE, CD19-PE, DX5-PE, CD11b-FITC (eBioscience), and CD11c-FITC (BioLegend) and sorted by a FACSAria II (BD). The purity of sorted cells were >96%.

Construction and expression. Mouse INAM cDNA (A630077B13Rik) was obtained from RIKEN and placed into expression vector pEFBOS and pLenti-IRES-hrGFP, both of which provide the specialized components needed for expression of a recombinant C-terminal FLAG fusion (Akazawa et al., 2007a). For construction of shRNA-expressing lentivirus vector, The ClaI–XhoI fragment of pLenti6-blockit-dest (Invitrogen) was inserted into pLenti-IRES-hrGFP at the site of ClaI and XhoI. This vector was named pLenti-dest-IRES-hrGFP (pLDIG). INAM sequence 5′-CTTCTCTCCG-GTTAGTTATCT-3′ was targeted for INAM knockdown (shINAM/pLDIG) and 5′-AGTCTGACATACTTATACTTA-3′ was used for negative control (shCont/pLDIG). We used a gene-expression kit, Lentiviral system (Invitrogen), as previously described (Akazawa et al., 2007a). Four plasmids (one of the pLenti vectors, pLP1, pLP2, and pLP/VSVG) were transfected into 293 FT packaging cells, and the viral particles for transfection were prepared according to the manufacturer's protocol. The 100× concentrated virus particles were produced after centrifugation of 8,000 *g* at 4°C for 16 h. Lentivirus produced by pLenti-IRES-hrGFP and pLDIBG could be tittered by GFP expression using flow cytometry. Because the lentivirus vector pLenti-IRES-hrGFP has the IRES-GFP region, we prepared negative control virus by pLenti-IRES-hrGFP without construct. Infection efficiency for BMDC was high with the control vector compared with the INAM-expressing lentivector (Fig. S6 A).

Real-time PCR. BMDCs were harvested after 4 h of stimulation by 100 ng/ml LPS, 50 μg/ml polyI:C, 1 μg/ml Pam_3CSK_4 (Pam3), 100 nM mycoplasmal macrophage-activating lipopeptide-2 (Malp-2), 10 μg/ml CpG, and 2,000 IU/ml IFN-α (Ebihara et al., 2007). Mouse tissues (heart, stomach, small intestine, large intestine, lung, brain, muscle, liver, kidney, thymus, and spleen) were collected from C57BL/6. Splenocytes were stained with CD3-PE, CD19-PE, DX5-PE, CD11b-PE, CD11c-FITC, and PDCA1-PE (eBioscience) and sorted by FACSAria (BD). Purity was >98% in each population. For RNA extraction, we used the RNeasy kit (Invitrogen). After removal of genomic DNA by treatment with DNase, randomly primed cDNA strands were generated with Moloney mouse leukemia virus reverse transcription (Promega). RNA expression was quantified by quantitative RT-PCR with gene-specific primers (IL-15 forward, 5′-TTAACTGAGGCTGGCATTCATG-3′; IL-15 reverse, 5′-ACCTACACTGACACAGCCCAAA-3′; INAM forward, 5′-CAACTGCAATGCCACGCTA-3′; INAM reverse, 5′-TCCAACC-GAACACCTGAGACT-3′; β-actin forward, 5′-TTTGCAGCTCCTTC-GTTGC-3′; β-actin reverse, 5′-TCGTCATCCATGGCGAACT-3′; HPRT forward, 5′-GTTGGATACAGGCCAGACTTTGTTG-3′; and HPRT reverse, 5′-GAAGGGTAGGCTGGCCTATAGGCT-3′) and values were normalized to the expression of β-actin mRNA or HPRT mRNA.

Other primers for PCR were designed using Primer Express software (Applied Biosystems) for another experiment. The following primers were used for PCR: β-actin forward, 5′-CCTGGCACCCAGCACAAT-3′ and reverse, 5′-GCCGATCCACACGGAGTACT-3′; granzyme B forward, 5′-TCCTGCTACTGCTGACCTTGTC-3′ and reverse, 5′-ATGATCTC-CCCTGCCTTTGTC-3′; IFN-α4 forward, 5′-CTGCTGGCTGTGAG-GACATACT-3′ and reverse, 5′-AGGCACAGAGGCTGTGTTTCTT-3′; TRAIL (Tnfsf10) forward, 5′-CTTCACCAACGAGATGAAGCAG-3′ and reverse, 5′-TCCGTCTTTGAGAAGCAAGCTA-3′; and IL-12p40 (Il12b), forward, 5′-AATGTCTGCGTGCAAGCTCA-3′ and reverse, 5′-ATGCCCACTTGCTGCATGA-3′.

Anti-INAM pAb. C-terminal INAM (cINAM; 191–314 aa) was subcloned between the NdeI and SalI sites of pColdI vector (Takara Bio Inc.). 6× His-tagged cINAM protein was expressed in BL21 by manufacturer's methods. The cells were sonicated in 20 mM Tris-HCl, 150 mM NaCL, 1 mM PMSF, and 7 M Urea, pH 7.4, on ice. Expression products of cINAM were purified using the HisTrap HP kit (GE Healthcare). The extracted proteins were refolded by stepwise dialysis against decreasing amounts of urea. Rabbit anti-cINAM polyclonal Ab was produced with the cINAM proteins by standard protocol. IgG was purified by precipitation with 33% ammonium sulfate, dialyzed against PBS.

Surface labeling with biotin. Biotinylation of cell surface proteins was performed according to the reported method (Tsuji et al., 2001). In brief, ~10^8 cells were suspended in 1 ml Hepes-buffered saline (HBS), pH 8.5, and incubated with 10 ml of 10 mg/ml NHS-sulfobiotin (Vector Laboratories) for 1 h at room temperature. Cells were washed in HBS three times and then solubilized with lysis buffer containing 1% NP-40, pH 7.4. The cell lysate was immunoprecipitated with avidin-labeled Abs as described previously (Tsuji et al., 2001).

Immunoblot analysis. Lysates were harvested 24 h after transfection of Flag-tagged INAM/pEFBOS into 293FT cells and treated with *N*-glycosidase F

Published November 8, 2010

(PNGaseF; New England Biolabs, Inc.) by the manufacturer's method in some experiments. Protein samples were separated on SDS-PAGE and immunoblotted by anti-Flag M2 Ab (Sigma-Aldrich). In some experiments, we used highly purified rabbit anti–mouse INAM polyclonal Ab for immunoblotting. The anti-INAM IgG was further purified with protein A–Sepharose and absorbed with BL21 bacterial lysate (where the INAM immunogen was produced) that contained no INAM peptide.

Confocal microscopy. BMDCs and NK cells were infected with control or INAM-expressing lentivirus as described previously (Akazawa et al., 2007a). 24 h later, cells were fixed with 4% paraformaldehyde for 30 min and permeabilized with PBS containing 0.5% saponin for 30 min at room temperature. Fixed cells were stained with anti-FLAG mAb and Alexa Fluor 568–conjugated secondary Ab. Stable Ba/F3 transfectants expressing INAM were treated with Cytofix/Cytoperm (BD) according to the manufacturer. Then cells were stained with PE-phalloidin and rabbit anti-INAM pAb followed by Alexa Fluor 488–conjugated secondary Ab. Cells were analyzed on a confocal microscope (LSM 510 META; Carl Zeiss, Inc.) for the detection of INAM.

BMDC–NK interaction. BMDCs were co-cultured with freshly isolated NK cells (BMDC/NK = ~1:2–1:5) with or without 10 μg/ml polyI:C for 24 h (Akazawa et al., 2007a). In some experiments, function of BMDCs and NK cells was modified by lentivirus vector before BMDC/NK co-culture. IRF-3$^{-/-}$ BMDCs were transfected by control lentivirus and INAM-expressing lentivirus (INAM/pLenti-IRES-hrGFP) and incubated with 6 μg/ml polybrene for 24 h before co-culture. WT BMDCs were transfected with shRNA-expressing lentivirus (shCont/pLDIG or shINAM/pLDIG) and incubated with 6 μg/ml polybrene for 48 h before co-culture. Freshly isolated NK cells were transfected with control lentivirus and INAM-expressing lentivirus (INAM/pLenti-IRES-hrGFP) and cultured with 6 μg/ml polybrene in the presence of 500 IU/ml IL-2 for 72 h before co-culture. Activation of NK cells was assessed by concentration of IFN-γ (ELISA; GE Healthcare) in the medium and by NK cytotoxicity against B16D8. Cytotoxicity was determined by standard ^{51}Cr release assay as described previously (Akazawa et al., 2007a).

Ex vivo NK activation. Mice were i.p. injected with 250 μg polyI:C. After 24 h, spleen cells were harvested and then NK cells (DX5$^+$ cells) were positively isolated with the MACS system (Miltenyi Biotec). The DX5$^+$ NK cells were suspended in RPMI1640 with 10% FCS and mixed with ^{51}Cr-labeled B16D8 cells at indicated E/T ratios. After 4 h, supernatants were harvested and ^{51}Cr release was measured. Specific lysis was calculated by (specific release − spontaneous release)/(max release − spontaneous release). In some experiments, blood was drawn from the eyes of mice 8 h after polyI:C administration for cytokine measurement.

Test for in vivo NK activation in LN. 5 × 10^5 WT BMDCs incubated with or without 10 μg/ml polyI:C for 24 h or 5 × 10^5 IRF-3$^{-/-}$ BMDCs infected with control virus or INAM-expressing lentivirus and allowed to stand for 24 h were injected into the footpads of WT C57BL/6 mice. 48 h later, cells in their inguinal LN were harvested, stained with PE-DX5, and sorted by FACSAria II. RNA was extracted from the DX5-positive cells with TRIzol.

DC therapy. DC therapy against mice with B16D8 tumor burden was described previously (Akazawa et al., 2007a). C57BL/6 mice (n = 3) were shaved at the flank and injected s.c. with 6 × 10^5 syngeneic B16D8 melanoma cells (indicated as day 0). For DC therapy, BMDCs were prepared by transfecting control lentivirus or INAM-expressing lentivirus (INAM/pLenti-IRES-hrGFP) and cultured for 24 h. At the time point indicated in the figures, 10^6 BMDCs were injected s.c. near the tumor. To deplete NK cells in vivo, mice were i.p. injected with hybridoma ascites of anti-NK1.1 mAb (PK136; Akazawa et al., 2007a). Tumor volumes were measured using a caliper every 1 or 2 d. Tumor volume was calculated using the formula: tumor volume (cm^3) = (long diameter) × (short diameter) × (short diameter) × 0.4.

Statistical analysis. Statistical analyses were made with the Student's t test. The p-value of significant differences is reported.

Online supplemental material. TICAM-1–inducible genes encoding putative membrane proteins relevant for this study are summarized in Table S1. Fig. S1 shows KO mice results suggesting that both IPS-1 and TICAM-1 in BMDC participate in polyI:C-driven NK activation. Data presented in Fig. S2 characterizes the in vivo polyI:C response of INAM in LN cells. Figs. S3 and S4 demonstrate the properties of surface-expressed INAM analyzed by immunoprecipitation/blotting and confocal microscopy, respectively. Fig. S5 mentions the cytokine expression and maturation profiles of INAM-overexpressing BMDC. Fig. S6 shows the effect of gene silencing of INAM on the polyI:C-mediated cytokine-inducing profile in BMDC. Two pieces of data presented in Fig. S7 confirm the presence of the INAM protein in INAM lentivirus-transduced BMDCs and NK cells. Online supplemental material is available at http://www.jem.org/cgi/content/full/jem.20091573/DC1.

We thank Drs. T. Akazawa and N. Inoue (Osaka Medical Center for Cancer, Osaka, Japan) for their valuable discussions. Thanks are also due to many discussions by our laboratory members. Particularly, extensive English review by Dr. Hussein H. Aly is gratefully acknowledged.

This project was supported by Grants-in-Aid from the Ministry of Education, Science, and Culture and the Ministry of Health, Labor, and Welfare of Japan, Mitsubishi Foundation, Mochida Foundation, NorthTec Foundation Waxman Foundation, and Yakult Foundation.

The authors declare no financial or commercial conflict of interest.

Submitted: 20 July 2009
Accepted: 13 October 2010

REFERENCES

Akazawa, T., T. Ebihara, M. Okuno, Y. Okuda, M. Shingai, K. Tsujimura, T. Takahashi, M. Ikawa, M. Okabe, N. Inoue, et al. 2007a. Antitumor NK activation induced by the Toll-like receptor 3-TICAM-1 (TRIF) pathway in myeloid dendritic cells. *Proc. Natl. Acad. Sci. USA.* 104:252–257. doi:10.1073/pnas.0605978104

Akazawa, T., M. Shingai, M. Sasai, T. Ebihara, N. Inoue, M. Matsumoto, and T. Seya. 2007b. Tumor immunotherapy using bone marrow-derived dendritic cells overexpressing Toll-like receptor adaptors. *FEBS Lett.* 581:3334–3340. doi:10.1016/j.febslet.2007.06.019

Azuma, M., R. Sawahata, Y. Akao, T. Ebihara, S. Yamazaki, M. Matsumoto, M. Hashimoto, K. Fukase, Y. Fujimoto, and T. Seya. 2010. The peptide sequence of diacyl lipopeptides determines dendritic cell TLR2-mediated NK activation. *PLoS One.* 5:e12550. doi:10.1371/journal.pone.0012550

Bertram, L., B.M. Schjeide, B. Hooli, K. Mullin, M. Hiltunen, H. Soininen, M. Ingelsson, L. Lannfelt, D. Blacker, and R.E. Tanzi. 2008. No association between CALHM1 and Alzheimer's disease risk. *Cell.* 135:993–994, author reply :994–996. doi:10.1016/j.cell.2008.11.030

Brandt, C.S., M. Baratin, E.C. Yi, J. Kennedy, Z. Gao, B. Fox, B. Haldeman, C.D. Ostrander, T. Kaifu, C. Chabannon, et al. 2009. The B7 family member B7-H6 is a tumor cell ligand for the activating natural killer cell receptor NKp30 in humans. *J. Exp. Med.* 206:1495–1503. doi:10.1084/jem.20090681

Brilot, F., T. Strowig, S.M. Roberts, F. Arrey, and C. Münz. 2007. NK cell survival mediated through the regulatory synapse with human DCs requires IL-15Ralpha. *J. Clin. Invest.* 117:3316–3329. doi:10.1172/JCI31751

Cerwenka, A., and L.L. Lanier. 2001. Natural killer cells, viruses and cancer. *Nat. Rev. Immunol.* 1:41–49. doi:10.1038/35095564

Cerwenka, A., A.B. Bakker, T. McClanahan, J. Wagner, J. Wu, J.H. Phillips, and L.L. Lanier. 2000. Retinoic acid early inducible genes define a ligand family for the activating NKG2D receptor in mice. *Immunity.* 12:721–727. doi:10.1016/S1074-7613(00)80222-8

Cerwenka, A., J.L. Baron, and L.L. Lanier. 2001. Ectopic expression of retinoic acid early inducible-1 gene (RAE-1) permits natural killer cell-mediated rejection of a MHC class I-bearing tumor in vivo. *Proc. Natl. Acad. Sci. USA.* 98:11521–11526. doi:10.1073/pnas.201238598

Dreses-Werringloer, U., J.C. Lambert, V. Vingtdeux, H. Zhao, H. Vais, A. Siebert, A. Jain, J. Koppel, A. Rovelet-Lecrux, D. Hannequin, et al. 2008. A polymorphism in CALHM1 influences Ca2+ homeostasis,

Abeta levels, and Alzheimer's disease risk. *Cell.* 133:1149–1161. doi:10.1016/j.cell.2008.05.048

Ebihara, T., H. Masuda, T. Akazawa, M. Shingai, H. Kikuta, T. Ariga, M. Matsumoto, and T. Seya. 2007. Induction of NKG2D ligands on human dendritic cells by TLR ligand stimulation and RNA virus infection. *Int. Immunol.* 19:1145–1155. doi:10.1093/intimm/dxm073

Fernandez, N.C., A. Lozier, C. Flament, P. Ricciardi-Castagnoli, D. Bellet, M. Suter, M. Perricaudet, T. Tursz, E. Maraskovsky, and L. Zitvogel. 1999. Dendritic cells directly trigger NK cell functions: cross-talk relevant in innate anti-tumor immune responses in vivo. *Nat. Med.* 5:405–411. doi:10.1038/7403

Fitzgerald, K.A., S.M. McWhirter, K.L. Faia, D.C. Rowe, E. Latz, D.T. Golenbock, A.J. Coyle, S.M. Liao, and T. Maniatis. 2003. IKKepsilon and TBK1 are essential components of the IRF3 signaling pathway. *Nat. Immunol.* 4:491–496. doi:10.1038/ni921

Gerosa, F., B. Baldani-Guerra, C. Nisii, V. Marchesini, G. Carra, and G. Trinchieri. 2002. Reciprocal activating interaction between natural killer cells and dendritic cells. *J. Exp. Med.* 195:327–333. doi:10.1084/jem.20010938

Hamerman, J.A., K. Ogasawara, and L.L. Lanier. 2004. Cutting edge: Toll-like receptor signaling in macrophages induces ligands for the NKG2D receptor. *J. Immunol.* 172:2001–2005.

Honda, K., H. Yanai, H. Negishi, M. Asagiri, M. Sato, T. Mizutani, N. Shimada, Y. Ohba, A. Takaoka, N. Yoshida, and T. Taniguchi. 2005. IRF-7 is the master regulator of type-I interferon-dependent immune responses. *Nature.* 434:772–777. doi:10.1038/nature03464

Hornung, V., S. Rothenfusser, S. Britsch, A. Krug, B. Jahrsdörfer, T. Giese, S. Endres, and G. Hartmann. 2002. Quantitative expression of toll-like receptor 1-10 mRNA in cellular subsets of human peripheral blood mononuclear cells and sensitivity to CpG oligodeoxynucleotides. *J. Immunol.* 168:4531–4537.

Huntington, N.D., N. Legrand, N.L. Alves, B. Jaron, K. Weijer, A. Plet, E. Corcuff, E. Mortier, Y. Jacques, H. Spits, and J.P. Di Santo. 2009. IL-15 trans-presentation promotes human NK cell development and differentiation in vivo. *J. Exp. Med.* 206:25–34. doi:10.1084/jem.20082013

Iwasaki, A., and R. Medzhitov. 2004. Toll-like receptor control of the adaptive immune responses. *Nat. Immunol.* 5:987–995. doi:10.1038/ni1112

Kalinski, P., R.B. Mailliard, A. Giermasz, H.J. Zeh, P. Basse, D.L. Bartlett, J.M. Kirkwood, M.T. Lotze, and R.B. Herberman. 2005. Natural killer-dendritic cell cross-talk in cancer immunotherapy. *Expert Opin. Biol. Ther.* 5:1303–1315. doi:10.1517/14712598.5.10.1303

Kato, H., O. Takeuchi, S. Sato, M. Yoneyama, M. Yamamoto, K. Matsui, S. Uematsu, A. Jung, T. Kawai, K.J. Ishii, et al. 2006. Differential roles of MDA5 and RIG-I helicases in the recognition of RNA viruses. *Nature.* 441:101–105. doi:10.1038/nature04734

Kawai, T., K. Takahashi, S. Sato, C. Coban, H. Kumar, H. Kato, K.J. Ishii, O. Takeuchi, and S. Akira. 2005. IPS-1, an adaptor triggering RIG-I- and Mda5-mediated type I interferon induction. *Nat. Immunol.* 6:981–988. doi:10.1038/ni1243

Kubin, M.Z., D.L. Parshley, W. Din, J.Y. Waugh, T. Davis-Smith, C.A. Smith, B.M. Macduff, R.J. Armitage, W. Chin, L. Cassiano, et al. 1999. Molecular cloning and biological characterization of NK cell activation-inducing ligand, a counterstructure for CD48. *Eur. J. Immunol.* 29:3466–3477. doi:10.1002/(SICI)1521-4141(199911)29:11<3466::AID-IMMU3466>3.0.CO;2-9

Lee, A.E., L.A. Rogers, J.M. Longcroft, and R.E. Jeffery. 1990. Reduction of metastasis in a murine mammary tumour model by heparin and polyinosinic-polycytidylic acid. *Clin. Exp. Metastasis.* 8:165–171. doi:10.1007/BF00117789

Levy, S., and T. Shoham. 2005. The tetraspanin web modulates immune-signalling complexes. *Nat. Rev. Immunol.* 5:136–148. doi:10.1038/nri1548

Lucas, M., W. Schachterle, K. Oberle, P. Aichele, and A. Diefenbach. 2007. Dendritic cells prime natural killer cells by trans-presenting interleukin 15. *Immunity.* 26:503–517. doi:10.1016/j.immuni.2007.03.006

Masuda, H., Y. Saeki, M. Nomura, K. Shida, M. Matsumoto, M. Ui, L.L. Lanier, and T. Seya. 2002. High levels of RAE-1 isoforms on mouse tumor cell lines assessed by anti-"pan" RAE-1 antibody confer tumor susceptibility to NK cells. *Biochem. Biophys. Res. Commun.* 290:140–145. doi:10.1006/bbrc.2001.6165

Matsumoto, M., and T. Seya. 2008. TLR3: interferon induction by double-stranded RNA including poly(I:C). *Adv. Drug Deliv. Rev.* 60:805–812. doi:10.1016/j.addr.2007.11.005

McCartney, S., W. Vermi, S. Gilfillan, M. Cella, T.L. Murphy, R.D. Schreiber, K.M. Murphy, and M. Colonna. 2009. Distinct and complementary functions of MDA5 and TLR3 in poly(I:C)-mediated activation of mouse NK cells. *J. Exp. Med.* 206:2967–2976. doi:10.1084/jem.20091181

Medzhitov, R., and C.A. Janeway Jr. 1997. Innate immunity: the virtues of a nonclonal system of recognition. *Cell.* 91:295–298. doi:10.1016/S0092-8674(00)80412-2

Meylan, E., J. Curran, K. Hofmann, D. Moradpour, M. Binder, R. Bartenschlager, and J. Tschopp. 2005. Cardif is an adaptor protein in the RIG-I antiviral pathway and is targeted by hepatitis C virus. *Nature.* 437:1167–1172. doi:10.1038/nature04193

Miyake, T., Y. Kumagai, H. Kato, Z. Guo, K. Matsushita, T. Satoh, T. Kawagoe, H. Kumar, M.H. Jang, T. Kawai, et al. 2009. Poly I:C-induced activation of NK cells by CD8 alpha+ dendritic cells via the IPS-1 and TRIF-dependent pathways. *J. Immunol.* 183:2522–2528. doi:10.4049/jimmunol.0901500

Mukai, M., F. Imamura, M. Ayaki, K. Shinkai, T. Iwasaki, K. Murakami-Murofushi, H. Murofushi, S. Kobayashi, T. Yamamoto, H. Nakamura, and H. Akedo. 1999. Inhibition of tumor invasion and metastasis by a novel lysophosphatidic acid (cyclic LPA). *Int. J. Cancer.* 81:918–922. doi:10.1002/(SICI)1097-0215(19990611)81:6<918::AID-IJC13>3.0.CO;2-E

Newman, K.C., and E.M. Riley. 2007. Whatever turns you on: accessory-cell-dependent activation of NK cells by pathogens. *Nat. Rev. Immunol.* 7:279–291. doi:10.1038/nri2057

Nomura, M., Z. Zou, T. Joh, Y. Takihara, Y. Matsuda, and K. Shimada. 1996. Genomic structures and characterization of Rae1 family members encoding GPI-anchored cell surface proteins and expressed predominantly in embryonic mouse brain. *J. Biochem.* 120:987–995.

Ohteki, T., H. Tada, K. Ishida, T. Sato, C. Maki, T. Yamada, J. Hamuro, and S. Koyasu. 2006. Essential roles of DC-derived IL-15 as a mediator of inflammatory responses in vivo. *J. Exp. Med.* 203:2329–2338. doi:10.1084/jem.20061297

Oshiumi, H., M. Matsumoto, K. Funami, T. Akazawa, and T. Seya. 2003a. TICAM-1, an adaptor molecule that participates in Toll-like receptor 3-mediated interferon-beta induction. *Nat. Immunol.* 4:161–167. doi:10.1038/ni886

Oshiumi, H., M. Sasai, K. Shida, T. Fujita, M. Matsumoto, and T. Seya. 2003b. TIR-containing adapter molecule (TICAM)-2, a bridging adapter recruiting to toll-like receptor 4 TICAM-1 that induces interferon-beta. *J. Biol. Chem.* 278:49751–49762. doi:10.1074/jbc.M305820200

Sasai, M., M. Shingai, K. Funami, M. Yoneyama, T. Fujita, M. Matsumoto, and T. Seya. 2006. NAK-associated protein 1 participates in both the TLR3 and the cytoplasmic pathways in type I IFN induction. *J. Immunol.* 177:8676–8683.

Sato, M., H. Suemori, N. Hata, M. Asagiri, K. Ogasawara, K. Nakao, T. Nakaya, M. Katsuki, S. Noguchi, N. Tanaka, and T. Taniguchi. 2000. Distinct and essential roles of transcription factors IRF-3 and IRF-7 in response to viruses for IFN-alpha/beta gene induction. *Immunity.* 13:539–548. doi:10.1016/S1074-7613(00)00053-4

Seth, R.B., L. Sun, C.K. Ea, and Z.J. Chen. 2005. Identification and characterization of MAVS, a mitochondrial antiviral signaling protein that activates NF-kappaB and IRF 3. *Cell.* 122:669–682. doi:10.1016/j.cell.2005.08.012

Seya, T., and M. Matsumoto. 2009. The extrinsic RNA-sensing pathway for adjuvant immunotherapy of cancer. *Cancer Immunol. Immunother.* 58:1175–1184. doi:10.1007/s00262-008-0652-9

Sivori, S., M. Falco, M. Della Chiesa, S. Carlomagno, M. Vitale, L. Moretta, and A. Moretta. 2004. CpG and double-stranded RNA trigger human NK cells by Toll-like receptors: induction of cytokine release and cytotoxicity against tumors and dendritic cells. *Proc. Natl. Acad. Sci. USA.* 101:10116–10121. doi:10.1073/pnas.0403744101

Tanaka, H., Y. Mori, H. Ishii, and H. Akedo. 1988. Enhancement of metastatic capacity of fibroblast-tumor cell interaction in mice. *Cancer Res.* 48:1456–1459.

Tsuji, S., J. Uehori, M. Matsumoto, Y. Suzuki, A. Matsuhisa, K. Toyoshima, and T. Seya. 2001. Human intelectin is a novel soluble lectin that recognizes galactofuranose in carbohydrate chains of bacterial cell wall. *J. Biol. Chem.* 276:23456–23463. doi:10.1074/jbc.M103162200

Vivier, E., E. Tomasello, M. Baratin, T. Walzer, and S. Ugolini. 2008. Functions of natural killer cells. *Nat. Immunol.* 9:503–510. doi:10.1038/ni1582

Xu, L.G., Y.Y. Wang, K.J. Han, L.Y. Li, Z. Zhai, and H.B. Shu. 2005. VISA is an adapter protein required for virus-triggered IFN-beta signaling. *Mol. Cell.* 19:727–740. doi:10.1016/j.molcel.2005.08.014

Yamamoto, M., S. Sato, H. Hemmi, K. Hoshino, T. Kaisho, H. Sanjo, O. Takeuchi, M. Sugiyama, M. Okabe, K. Takeda, and S. Akira. 2003a. Role of adaptor TRIF in the MyD88-independent toll-like receptor signaling pathway. *Science.* 301:640–643. doi:10.1126/science.1087262

Yamamoto, M., S. Sato, H. Hemmi, S. Uematsu, K. Hoshino, T. Kaisho, O. Takeuchi, K. Takeda, and S. Akira. 2003b. TRAM is specifically involved in the Toll-like receptor 4-mediated MyD88-independent signaling pathway. *Nat. Immunol.* 4:1144–1150. doi:10.1038/ni986

Yoneyama, M., M. Kikuchi, T. Natsukawa, N. Shinobu, T. Imaizumi, M. Miyagishi, K. Taira, S. Akira, and T. Fujita. 2004. The RNA helicase RIG-I has an essential function in double-stranded RNA-induced innate antiviral responses. *Nat. Immunol.* 5:730–737. doi:10.1038/ni1087

Zanoni, I., M. Foti, P. Ricciardi-Castagnoli, and F. Granucci. 2005. TLR-dependent activation stimuli associated with Th1 responses confer NK cell stimulatory capacity to mouse dendritic cells. *J. Immunol.* 175:286–292.

Zou, Z., M. Nomura, Y. Takihara, T. Yasunaga, and K. Shimada. 1996. Isolation and characterization of retinoic acid-inducible cDNA clones in F9 cells: a novel cDNA family encodes cell surface proteins sharing partial homology with MHC class I molecules. *J. Biochem.* 119:319–328.

Published November 8, 2010

JEM

SUPPLEMENTAL MATERIAL

Ebihara et al., http://www.jem.org/cgi/content/full/jem.20091573/DC1

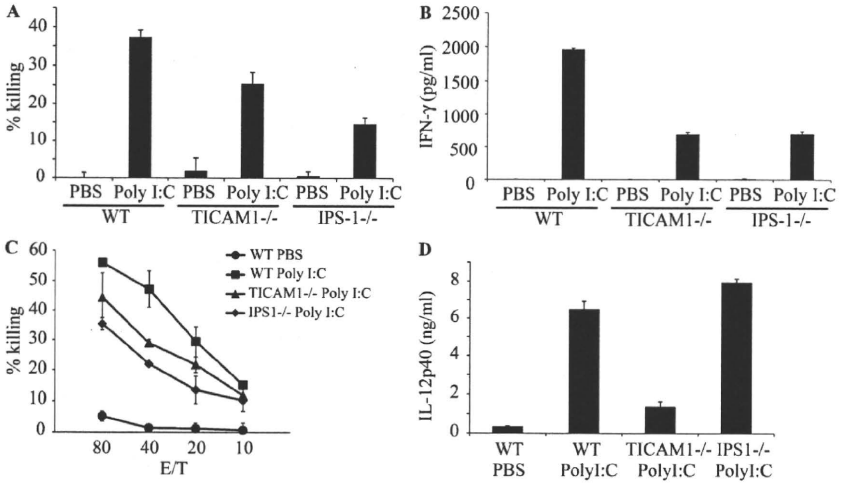

Figure S1. KO mice results suggest that both IPS-1 and TICAM-1 in BMDC participate in polyI:C-driven NK activation. (A and B) IPS-1 and TICAM-1 in BMDC participate in polyI:C-driven NK activation. 2.5 × 10^5 BMDCs prepared from WT, TICAM1$^{-/-}$, and IPS1$^{-/-}$ mice were incubated with 5 × 10^5 NK cells in the presence or absence (PBS) of 50 µg/ml polyI:C for 24 h. Then, the supernatants were harvested for IFN-γ ELISA (B). To determine NK cytotoxicity, ^{51}Cr-labeled B16D8 cells were added to the culture and, 4 h later, released ^{51}Cr was measured (A). One representative of three similar experiments is shown. (C) Both IPS-1 and TICAM-1 participate in in vivo polyI:C-induced NK activation. WT, IPS-1$^{-/-}$, and TICAM-1$^{-/-}$ mice were i.p. injected with 250 µg polyI:C. After 24 h, NK cells were harvested by DX5-MACS beads from spleen and used as effector cells in a cytotoxic assay with ^{51}Cr-labeled B16D8 targets. Cytotoxic activity of NK cells was measured under the indicated E/T ratios 4 h after the E/T mixing. One representative of the three similar experiments is shown. (D) Increasing serum level of IL-12p40 is dependent on TICAM-1. 250 µg polyI:C was i.p. injected into a series of mice as in B. 8 h after injection of polyI:C, blood serum was collected to determine the levels of IL-12p40 by ELISA. Although it is not depicted, IL-12p70 was not detected in these samples by ELISA. Data in A–D represent mean ± SD.

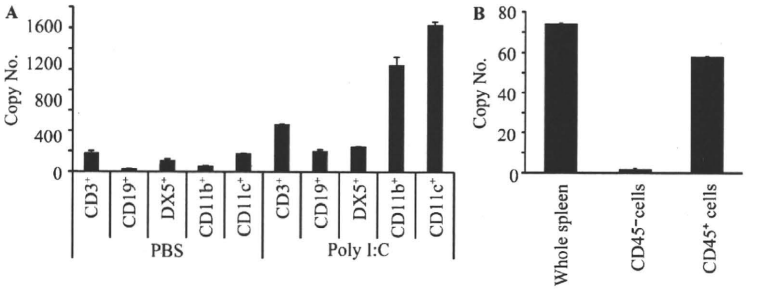

Figure S2. In vivo polyI:C response of INAM in LN cells. (A) Up-regulation of INAM expression in LN cells by polyI:C injection. WT C57BL/6 mice were i.p. injected with 100 µg polyI:C or control buffer. After 24 h, inguinal, axillary, and mesenteric LN were harvested. Cell populations with indicated markers were separated by FACS sorting, and the INAM mRNA level of each population was determined by real-time PCR. (B) CD45$^+$ cells express INAM. Splenocytes were separated into CD45$^-$ and CD45$^+$ cells after the polyI:C injection as in A. The INAM mRNA levels of the two populations were determined by real-time PCR. Representative data from one of three experiments are shown. Data in A and B represent mean ± SD.

Published November 8, 2010

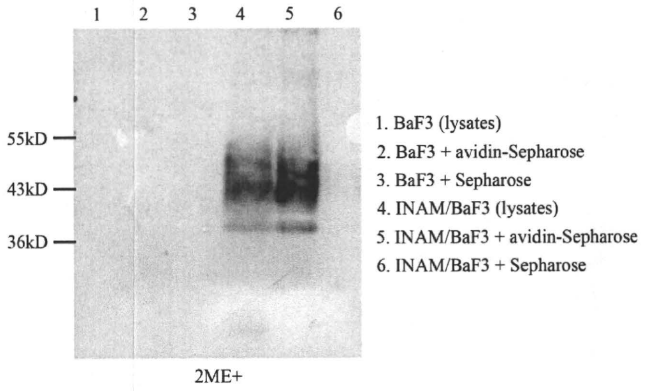

Figure S3. INAM is expressed on cell surface. Membrane proteins of Flag-tagged INAM-expressing BaF3 (INAM/BaF3) and control BaF3 were biotinylated and solubilized. Biotinylated proteins were immunoprecipitated by Avidin-Sepharose or control Sepharose. After electrophoresis on SDS-PAGE, INAM was detected by anti-Flag M2 mAb.

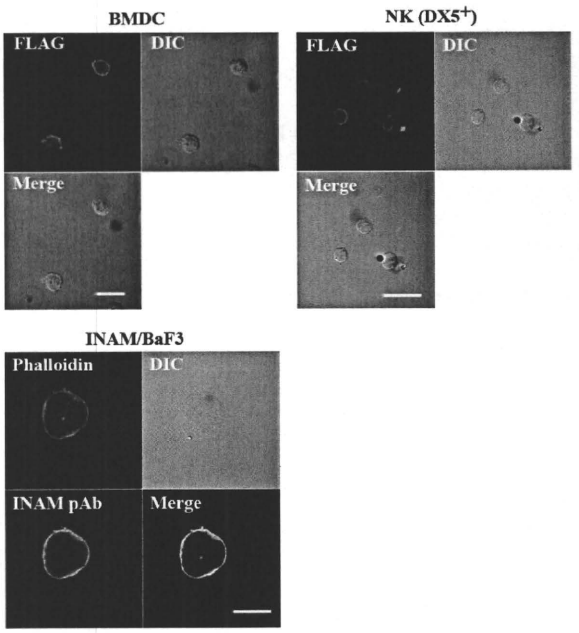

Figure S4. Confocal analysis of surface-expressed INAM. WT BMDC (left) or NK cells (right) were infected with INAM-expressing vector and stained with anti-FLAG mAb (Alexa Fluor 568). Stable Ba/F3 transfectants expressing INAM (bottom) were permeabilized and stained with phalloidin and anti-INAM pAb, followed by Alexa Fluor 488–conjugated secondary antibody. Cells were analyzed on a confocal laser-scanning microscope (LSM 510 META). Bars, 20 μm.

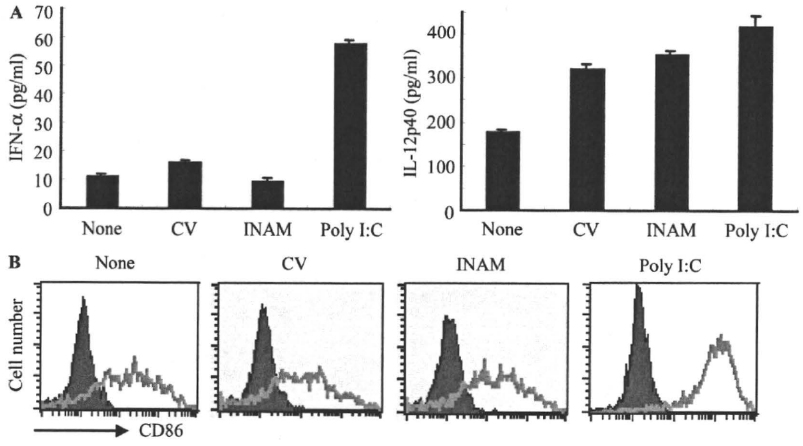

Figure S5. INAM-overexpressing BMDC did not induce cytokine responses and maturation. WT BMDCs were transfected with control lentivirus (CV) or INAM-expressing lentivirus (INAM-virus) and cultured for 24 h. (A) ELISA of IFN-α and IL-12p40 in the culture supernatants. Data shown are means ± SD of triplicate samples from one experiment representative of three. (B) Flow cytometry for CD86 in the transfected BMDC. Polyl:C stimulation (10 μg/ml) was used for positive control.

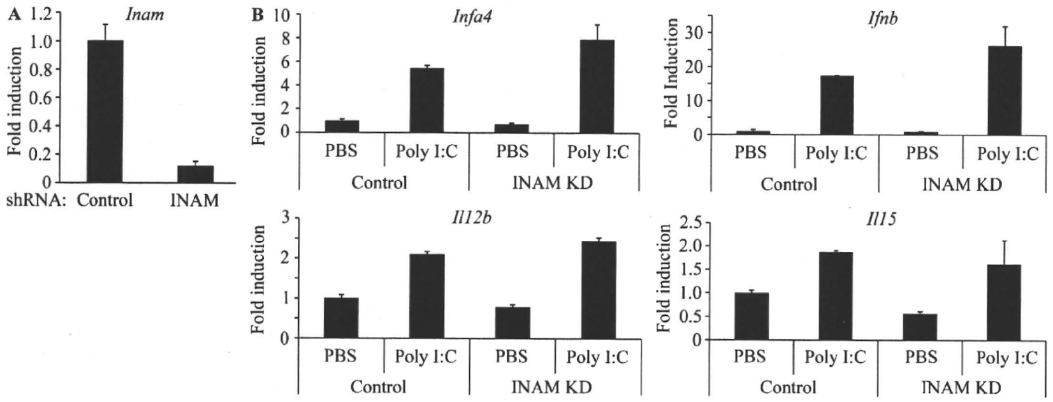

Figure S6. The effect of gene silencing of INAM on the polyI:C-mediated cytokine inducing profile in BMDC. (A) Gene silencing of INAM in BMDC. 5 × 10^5 WT BMDCs were infected with INAM shRNA-generating lentivirus or control lentivirus. After 36 h, the levels of INAM mRNA expression were assessed by real time PCR. Data show one of three similar experiments. (B) Effect of BMDC INAM on cytokine expression. INAM in 5 × 10^5 WT BMDCs was silenced as in A. Then, control or INAM-silenced BMDC were stimulated with 10 μg/ml polyI:C for 8 h. RNA was harvested from BMDC with RNeasy and the levels of indicated mRNA were determined by real-time PCR. Data show one of two similar experimental results. Data in A and B represent mean ± SD.